Manuscript Title: Robust timetable optimization for bus lines subject to resource and regulatory constraints

Journal Article DOI: https://doi.org/10.1016/j.tre.2019.05.016

To be cited as: Gkiotsalitis, K., & Alesiani, F. (2019). Robust timetable optimization for bus lines subject to resource and regulatory constraints. *Transportation Research Part E: Logistics and Transportation Review*, vol. 128, 30-51.

Robust timetable optimization for bus lines subject to resource and regulatory constraints

K.Gkiotsalitis[a,1,*], F.Alesiani[b]

[a] *University of Twente, Center for Transport Studies, Horst - Ring Z-222, P.O. Box 217, 7500 AE Enschede, The Netherlands*
[b] *NEC Laboratories Europe, Kurfürsten-Anlage 36, 69115 Heidelberg, Germany*

Abstract

Timetables are typically generated based on passenger demand and travel time expectations. This work incorporates the travel time and passenger demand uncertainty to generate robust timetables that minimize the possible loss at worst-case scenarios. We solve the resulting minimax problem with a genetic algorithm that uses sequential quadratic programming to evaluate the worst-case performance of each population member. Our approach is tested on a bus line in Singapore demonstrating an improvement potential of $\simeq 5\%$ on service regularity and excessive trip travel times.

Keywords: Bus scheduling; Robust timetabling; Dispatching time determination; High-frequency services; Service regularity

1. Introduction

The rapid adoption of telematics and fare collection systems from bus operators has improved the monitoring and reliability of transit services (Pangilinan et al., 2008). Public transport authorities use monitoring to penalize (reward) underperforming (overperforming) bus operators with direct monetary incentives (Jansson and Pyddoke, 2010). As an example, the introduced Bus Service Reliability Framework (BSRF) in Singapore provides to bus operators 2,000 Singaporean dollars per month for every 6-second improvement of the passenger excess waiting times (EWT) (Leong et al., 2016). This has motivated bus operators to improve their daily operations by incorporating new forms of user-generated data such as social media (Grant-Muller et al. (2014); Gkiotsalitis and Stathopoulos (2015); Chaniotakis and Antoniou (2015); Gkiotsalitis and Stathopoulos (2016)), cellular (Toole et al. (2015); Calabrese et al. (2015)) or Automated Fare Collection (AFC) data (Uniman et al., 2010).

User-generated data can be used at the strategic planning and the tactical planning which consists of the (i) frequency setting; (ii) timetable design and (iii) vehicle and crew scheduling (Ceder (2007); Farahani et al. (2013); Gkiotsalitis et al. (2019)). For instance, Gkiotsalitis and Cats (2018) set reliable frequencies for the bus services in central Stockholm using insights from operational automated vehicle location (AVL) and AFC data.

*Corresponding author
Email addresses: k.gkiotsalitis@utwente.nl (K.Gkiotsalitis), francesco.alesiani@neclab.eu (F.Alesiani)
[1]Tel.: +31 534 891 870

Along the same lines, Wang et al. (2017) developed data-driven timetables using smart-card records. There is also a distinct line of recent works in rail and metro operations that use different forms of user-generated data to improve the strategic and tactical planning (Niu et al., 2015a,b; Sels et al., 2016; Yang et al., 2017; Yin et al., 2018; Sun et al., 2018).

Besides the strategic and tactical planning, bus operators are also willing to improve their operational planning. For instance, bus operators occasionally deploy a variety of near real-time control measures such as stop-skipping (Sun and Hickman, 2005; Chen et al., 2015; Yu et al., 2015; Gkiotsalitis, 2019), bus holding (Newell, 1974; Hernández et al., 2015; Wu et al., 2017; Gkiotsalitis and Cats, 2019) and short-turnings (Zhang et al., 2017) to recover from exogenous disruptions. Nevertheless, those corrective measures can inflict undesirable secondary effects such as an increase of in-vehicle travel times due to bus holding (Fu and Yang, 2002); deadheading times due to short-turning (Gkiotsalitis and Maslekar, 2018a); and, missed boardings due to stop-skipping (Liu et al., 2013). Other potential undesirable effects are the disruptions of crew and vehicle schedules and "schedule sliding" where future trips are delayed.

Given the negative effects of the corrective control measures during the actual operations, this study focuses on the improvement of timetables at the tactical planning stage. One of the main problems in the generation of timetables is the uncertain nature of trip travel times and passenger demand. That is, timetables that plan the dispatching times of daily trips based on the historical averages of trip travel times and passenger demand result in services that underperform even under the presence of slight disruptions (Ibarra-Rojas et al., 2015). As a remedy, other approaches generate timetables based on stochastic optimization methods by using the estimated probability distributions of travel times and passenger demand. Such timetables tend to perform well on cases which are close to the average, but unsatisfactory at the low-probability regions of the probability distributions (Marzat et al., 2016). That is, such timetables are ineffective in the case of less common disruptions. This motivates our work: we propose an evolutionary optimization method that can generate robust timetables which perform well even in worst-case scenarios of travel time and passenger demand disturbances.

The potential benefit of robust timetables is twofold: (i) they do not require the estimation of probability distributions for the passenger demand and the interstation travel times of all trips - which is a laborious task; and (ii) their performance can be satisfactory even at worst-case scenarios that appear at the low-probability regions of the probability distributions. We define robust timetables as timetables that maintain their operational performance in worst-case scenarios of passenger demand and travel time disturbances. Their importance was highlighted by Gkiotsalitis and Kumar (2018) who showed that timetables based on demand/travel time averages or stochastic optimization were counterproductive when the actual travel times varied by more than 30% from their expected values. This was also one of the main conclusions in the survey paper of Ibarra-Rojas et al. (2015) which proposed the use of historical AVL and automated passenger counting (APC) data to develop robust timetables that can cope with the uncertainty of the bus operations. Our work contributes to this line of research by developing a method for robust timetable optimization. To this end, we incorporate the inherent uncertainty of travel times and passenger demand in the generation of timetables and introduce a genetic algorithm that uses sequential quadratic programming to solve the resulting minimax problem. In our experiments at a service line in Singapore, we demonstrate an

improvement potential of $\simeq 5\%$ on service regularity and excessive trip travel times.

The remainder of this paper is structured as follows: in the next section, we provide a review of related works and highlight the contributions of this study. Section 3 models the movement of buses by considering the travel times. This model is used in section 4 together with practical operational constraints to form a mathematical program for the timetabling problem. The robust timetable problem is reformulated in section 5 to relax the inequality constraints that cannot be satisfied in all cases. A solution method is presented in section 6. Experimental results from a service line in Singapore are presented in section 7.

2. Related works on timetable optimization

A distinct line of works has proposed the simultaneous optimization of the route network design, the frequency setting, and the timetabling problems (Yan et al., 2006; Zhao and Zeng, 2008). Other works, such as Furth and Wilson (1981); Gallo and Miele (2001); Peeters and Kroon (2001) and Ávila-Torres et al. (2017), proposed the simultaneous optimization of bus frequencies and timetables. Contrary to the above, most works on timetable optimization, such as Sun et al. (2015); Wang et al. (2017) and Yu et al. (2017), decouple the frequency settings problem from the timetabling problem and solve them in sequential order.

Ceder et al. (2001); Cevallos and Zhao (2006); Wei and Sun (2017) and Gkiotsalitis and Maslekar (2018b) concentrate on timetable synchronization to minimize the waiting times of passengers at transfer stops. The seminal work of Ceder et al. (2001) was later extended by Eranki (2004) and Ibarra-Rojas and Rios-Solis (2012) to develop flexible timetables that provide some buffer time at the synchronization (transfer) points to cope with operational delays. Lately, Kang et al. (2019) developed a last train and bus bridging coordination model to mitigate the number of stranded passengers by the last train of the day. Along the same lines, Guo et al. (2018) proposed a mixed integer programming model to smoothen the synchronization from rail first-trains to the bus service. Nevertheless, the line of research that considers transfer synchronizations is not the primary focus of this work; thus, we will not expand further on this topic.

Another line of works embeds proactively slack times in the daily trips to add flexibility during the operations. Introducing long slack times though requires more buses to maintain the same service frequency. Adamski and Turnau (1998), Zhao et al. (2006) and Daganzo (2009) studied this problem and introduced robust optimization methods to calculate efficient slack times.

Other works on timetable optimization strive to ensure that the dispatching times of trips are evenly-spaced throughout the day. For instance, Ceder (2011) and Ceder et al. (2013) strive to achieve a desired even-load level for all buses at their maximum loading point by determining trip dispatching times that do not deviate significantly from the desired even headways. Similarly, Daduna and Voß (1995) and Shafahi and Khani (2010) generated timetables with evenly-spaced dispatching times incorporating the additional objective of synchronizing passenger transfers.

Another classification of the literature in timetable optimization is the categorization into works that use deterministic travel and dwell times during the optimization process and works that use stochastic ones. The latter body of works is closer to our work which uses historical AVL and APC data to generate robust timetables. One example

of such works is the work of Wu et al. (2015) which assumed stochastic bus travel times to calculate slack times at transfer stops and improve the synchronization of timetables. Studies on operational control have also considered stochastic travel times. Xuan et al. (2011) used stochastic travel times to derive dynamic bus holding strategies and improve adherence to the planned schedule. Additionally, Hickman (2001) developed an analytical bus holding model that considers stochastic link travel times and boardings/alightings. Such works, use a typical probability distribution that approximates the stochastic nature of travel times and find a solution by solving a stochastic optimization problem.

Estimating probability distributions that are representative of the stochastic nature of travel times and demand is not an easy task. The recent works of Hans et al. (2015a,b) showed that the shapes of typical probability distributions (normal, log-normal and Gamma distributions) that have been predominantly used to fit the observed interstation travel times (see Andersson and Scalia-Tomba (1981); Daganzo (2009)) do not exhibit good performance. Hans et al. (2015b) calibrated the parameters of the above-mentioned probability distributions for each link using the maximum likelihood estimation (MLE) method and found that (i) the typically used probability distributions do not perform well (i.e., they are inferior to manually refined distributions) and (ii) their fitness varies significantly from case to case leading to a laborious calibration effort.

Other common problems with commonly used stochastic optimization approaches are: (i) estimating the probability distributions of travel times and passenger demand is a laborious task; (ii) the fitted probability distributions for a particular bus line cannot be generalized to other lines leading to numerous, repeated calibrations; and (iii) the performance of the resulting timetable is unsatisfactory if the realized travel and dwell times are at the low-probability regions of the fitted probability distributions (Marzat et al., 2016).

As a remedy, this work considers the uncertain nature of travel times and passenger demand and seeks timetable solutions that perform well even at worst-case scenarios. This work is different from the above-mentioned works because it does not use probability distributions to approximate the observed travel times and passenger demand. Instead, we use uncertainty sets within which we can have any kind of passenger demand and travel time disruption. To model this, we introduce a bus movement model that incorporates the uncertainty of travel times and passenger demand. The resulting robust timetable minimizes the possible loss at a worst-case scenario and is determined by the introduction of a solution method based on evolutionary optimization and sequential quadratic programming.

The incremental contribution(s) of this work to the state-of-the-art are: (a) the consideration of in-vehicle times as a problem objective to avoid prolonging trip travel times that appear in other works (see Fu and Yang (2002)); (b) the development of a timetable optimization model that uses (bounded) uncertainty sets of travel times and passenger demand, instead of typical probability distributions (Hickman, 2001; Wu et al., 2015); and (c) the inclusion of practical, regulatory constraints in the generation of the timetable such as the resting times of bus drivers, the required deadheading times and the maximum dispatching headway limits.

3. Modeling the movement of buses

3.1. Assumptions

The main assumptions of this work are:

(1) Link travel times, where a link is considered as the road segment between two consecutive bus stops, are time-dependent and they are related to the time of the day when the link is traversed (as in several other works such as the work of Wang et al. (2017)).

(2) Passenger arrivals at stops are random (follow the uniform distribution). This is a common assumption for high-frequency services (see Welding (1957); Randall et al. (2007)) where the headways are so small that passengers cannot coordinate their arrivals at stops with the arrivals of buses.

(3) The determined frequencies (that precede the timetabling stage) ensure that the load of the buses does not exceed the capacity. This is a reasonable assumption since frequencies are determined such that all passengers at the maximum load point of the line can be accommodated (Vuchic, 2017).

3.2. Movement modeling

To consider the temporal variations of the link travel times, we partition a day into even time periods $T = \{1, ..., \tau, ..., |T|\}$. Each link travel time is stochastic, and the domain of its values depends on the time the link is traversed (time-dependent link travel time). We can assign any time of the day, $\mathcal{T}$, to a time period $\tau = \left\lceil \frac{|T|}{86400} \mathcal{T} \right\rceil$, where $\mathcal{T}$ is expressed in seconds.

The scheduled dispatching time g_n of each daily trip $n \in N$ (where N is the set of all daily trips) is determined from the frequency settings phase. In this work, we explore the possibility of defining robust timetables with uneven trip dispatching times. That is, we allow a deviation (offset) x_n from each originally scheduled dispatching time g_n.

The dispatching time deviations of all daily trips, $\boldsymbol{x} \in \mathbb{Z}^{|N|}$, are the decision variables because they modify the originally planned dispatching times, g_n, to increase the robustness of the timetable. Each element from vector $\boldsymbol{x} = \{x_1, ..., x_n, ..., x_{|N|}\}$ expresses the dispatching time offset in minutes and is an integer number. To describe the main components of the robust timetabling problem, we introduce the notation in Table 1.

When modeling the movement of a bus trip n in time and space, the departure time of any bus trip $n \in N \setminus \{1\}$ from any bus stop s is equal to the arrival time, $a_{n,s}(\boldsymbol{x})$, plus the dwell time, $k_{n,s}(\boldsymbol{x})$:

$$d_{n,s}(\boldsymbol{x}) = \begin{cases} g_n + x_n \text{ if } s = 1 \\ a_{n,s}(\boldsymbol{x}) + k_{n,s}(\boldsymbol{x}),\ \forall s > 1 \end{cases} \qquad \forall n \in N \setminus \{1\} \tag{1}$$

where

$$a_{n,s}(\boldsymbol{x}) = d_{n,s-1}(\boldsymbol{x}) + t_{s-1,\tau}\ \forall s \in S/\{1\} \text{ where } \tau = \left\lceil \frac{|T|}{86400} d_{n,s-1}(\boldsymbol{x}) \right\rceil \tag{2}$$

Table 1: Notation

Indices	
n	indexes of bus trips
s	indexes of bus stops
Sets	
$S = \{1, ..., s, ...\}$	set of ordered bus stops for the examined bus line
$N = \{1, ..., n, ...\}$	set of ordered trips for the examined bus line. The number of trips is defined already from the frequency settings stage
$R = \{1, ..., \varrho, ..., 24\}$	set of ordered hourly time periods of the day for modeling time-varying origin-destination matrices
$T = \{1, ..., \tau, ...\}$	set of temporal partition of the day into time periods for modeling time-varying link travel times
$Z = \{Z_1, ..., Z_i, ...\}$	discrete set of all possible dispatching time deviations from the originally planned dispatching times in minutes (or 60-second intervals)
$\mathcal{V}_{s,\tau}$ (sec)	uncertainty set from which the uncertain parameter $t_{s,\tau}$ can take any value
$\mathcal{U}_{s,\varrho}$ (pass./h)	uncertainty set from which the uncertain parameter $\beta_{s,\varrho}$ can take any value
Uncertain Parameters	
$\boldsymbol{\beta} = \{\beta_{s,\varrho}\}$ (pass./h)	$\beta_{s,\varrho}$ is the *uncertain* parameter of the boardings in passengers per hour at stop s for hour ϱ where ϱ is one of the 24 hours of the day
$\boldsymbol{t} = \{t_{s,\tau}\}$(sec)	$t_{s,\tau}$ is the *uncertain* parameter of the link travel time between consecutive stops s and $s+1$ for the time period τ
Parameters	
w_s (sec)	the planned headway at stop $s \in S$
c_n (pass.)	the capacity of bus trip n in number of passengers
φ_n (sec)	the layover time (the required break and deadhead time for a bus that completed its trip, n, before starting the next one)
$O_\varrho = \{o_{i,s,\varrho}\}$ (%)	$o_{i,s,\varrho}$ is the percentage of boarded passengers at stop $i < s$ that will alight at stop s when the boardings at stop i occurred within the hourly period ϱ
b_n (unitless)	b_n returns the trip number of the previous bus trip that was operated by the same bus as trip $n \in N$
p_0 (sec)	the minimum time a bus is held at a bus stop if there are no boardings/alightings
p_1 (sec/pass.)	the time needed for each passenger boarding
p_2 (sec/pass.)	the time needed for each passenger alighting
g_{first} (sec)	the originally planned dispatching time of the first trip of the day
g_n (sec)	the originally planned dispatching time of each daily trip $n \in N$
H (sec)	a maximum limit of the dispatching headways of two subsequent buses to ensure a minimum level of service (sec)
Decision variables	
$\boldsymbol{x} = \{x_1, ..., x_n, ...\}$ (sec)	the dispatching time deviation from each originally planned dispatching time g_n. They can take any value from the discrete set Z
Variables	
$d_{n,s}(\boldsymbol{x})$ (sec)	the departure time of each bus trip $n \in N$ from stop $s \in S$
$a_{n,s}(\boldsymbol{x})$ (sec)	the arrival time of each bus trip $n \in N$ at stop $s \in S$
$h_{n,s}(\boldsymbol{x})$ (sec)	the headway at stop $s \in S$ between bus trip $n \in N$ and its leading bus trip n'
$k_{n,s}(\boldsymbol{x})$ (sec)	the dwell time of trip $n \in N$ at stop $s \in S$
$q_{n,s}(\boldsymbol{x})$ (pass.)	the number of passengers that board trip $n \in N$ at stop $s \in S$
$r_{n,s}(\boldsymbol{x})$ (pass.)	the number of alightings of trip $n \in N$ at stop $s \in S$
$l_{n,s}(\boldsymbol{x})$ (pass.)	the busload (defined as the total number of onboard passengers) for trip $n \in N$ at stop $s \in S$

The dwell time $k_{n,s}(\boldsymbol{x})$ of a bus trip n at stop s depends on the number of boardings and alightings (Kraft and Bergen (1974)). Detailed studies on estimating the dwell times such as Levinson (1983), Guenthner and Sinha (1983) and Bertini and El-Geneidy (2004) showed that the dwell time is equal to a minimum value that can range from 0-5 seconds in case of no boardings/alightings. This value increases by $1.5-4.5$ seconds for each extra passenger boarding and $1-2$ seconds for each passenger alighting depending on the fare payment structure. Selecting values of the parameters p_0, p_1 and p_2 from the above, yields the following dwell time expression:

$$k_{n,s}(\boldsymbol{x}) = k_n(q_{n,s}(\boldsymbol{x}), r_{n,s}(\boldsymbol{x})) = p_0 + \max\{p_1 q_{n,s}(\boldsymbol{x}), p_2 r_{n,s}(\boldsymbol{x})\} \tag{3}$$

Remark 1: Eq.3 assumes that the front door of the buses is used for passenger boardings and the back door for alightings. If passengers who are willing to board need to wait until the onboard passengers exit the bus, Eq.3 should be substituted by: $k_{n,s}(\boldsymbol{x}) = p_0 + p_1 q_{n,s}(\boldsymbol{x}) + p_2 r_{n,s}(\boldsymbol{x})$.

The passenger boardings at trip n and stop s are associated with the inter-departure time between trip n and its preceding trip n' at that stop. If passengers board trip n at stop s within the ϱ^{th} hour of the day, the number of passenger boardings is:

$$q_{n,s}(\boldsymbol{x}) := \frac{\beta_{s,\varrho}}{3600(\text{sec/hour})} \left(d_{n,s}(\boldsymbol{x}) - d_{n',s}(\boldsymbol{x})\right) \tag{4}$$

The alightings of trip n at stop s, $r_{n,s}(\boldsymbol{x})$, can be related to the actual passenger boardings at previous stops, $q_{n,i}(\boldsymbol{x})$ where $i = \{1, ..., s-1\}$, using the hourly $O_\varrho = \{o_{i,s,\varrho}\}$ origin-destination matrix. $o_{i,s,\varrho}$ is the percentage of boarded passengers at stop $i < s$ that will alight at stop s and can be used for defining the alightings:

$$r_{n,s}(\boldsymbol{x}) := \sum_{i=1}^{i=s-1} q_{n,i}(\boldsymbol{x}) o_{i,s,\varrho} \text{ where } \varrho = \left\lceil \frac{|R|}{86400} a_{n,i}(\boldsymbol{x}) \right\rceil \tag{5}$$

The term $\left\lceil \frac{|R|}{86400} a_{n,i}(\boldsymbol{x}) \right\rceil$ in eq.5 yields the hour-long time period, ϱ, within which the bus trip n arrived at stop i. In addition, $o_{i,s,\varrho}$ is the percentage of boarded passengers at stop $i < s$ that will alight at stop s for which $\sum_{s \in S} o_{i,s,\varrho} = 100\%$, $\forall i \in S, \varrho \in R$.

Furthermore, the passenger load of trip n after departing from any stop s can be expressed by the passenger flow conservation law:

$$l_{n,s}(\boldsymbol{x}) := \sum_{i=1}^{i=s} q_{n,i}(\boldsymbol{x}) - \sum_{i=1}^{i=s} r_{n,i}(\boldsymbol{x}) \tag{6}$$

The number of passenger boardings $q_{n,s}(\boldsymbol{x})$ can be used in eq.5 for deriving the number of alightings at the next stop, $s+1$. This information is used in eq.6 for deriving the busload at the current stop and in eq.3 for deriving the dwell time at the current stop.

The time headway $h_{n,s}(\boldsymbol{x})$ between bus trip n and its preceding bus trip n' upon their arrival at stop s is:

$$h_{n,s}(\boldsymbol{x}) := a_{n,s}(\boldsymbol{x}) - a_{n',s}(\boldsymbol{x}) \tag{7}$$

Note that if we do not have any overtaking(s), $n' = n - 1$ because the trips maintain their dispatching order.

Plugging eq.3, 7 and 2 into eq.1 yields the following bus movement expression:

$$\begin{aligned} d_{n,s}(\boldsymbol{x}) =& d_{n,s-1}(\boldsymbol{x}) + t_{s-1,\tau} + p_0 + \max\{p_1 q_{n,s}(\boldsymbol{x}), p_2 r_{n,s}(\boldsymbol{x})\} \\ & , \forall s \in S/\{1\},\ \forall n \in N/\{1\} \text{ where } \tau = \left\lceil \frac{|T|}{86400} d_{n,s-1}(\boldsymbol{x}) \right\rceil \end{aligned} \tag{8}$$

which is a recursive formula that can return the departure time of each bus trip from each bus stop. Expressing the departure time of buses with this recursive formula allows us to calculate the effect of the dispatching time deviations, $\boldsymbol{x}$, to those departure times. Later on, we can link the departure times with possible travel time and passenger boarding fluctuations to find a robust solution.

4. Modeling the objectives and the constraints of the timetabling problem

4.1. Constraints

4.1.1. Layover time constraint

The layover times are the required deadheading and recovery times of consecutive trips operated by the same bus. Minimum layover times are explicitly included in labor union contracts. A layover time can span from zero to several minutes depending on the resting time of the bus driver and the required turn-around time.

The layover time dictates that a bus trip b_n should spend at least a time period of $\varphi_{b_n} \geq 0$ seconds before starting its next trip, n. Therefore, the layover constraints for all daily trips are expressed as:

$$a_{b_n,|S|}(\boldsymbol{x}) + k_{b_n,|S|}(\boldsymbol{x}) + \varphi_{b_n} \leq g_n + x_n \quad \forall n \in N \setminus \{1\} \tag{9}$$

The above expression dictates that a bus trip n should be dispatched after the previous bus trip operated by the same bus is completed factoring in its layover time.

4.1.2. Constraining the dispatching times of the first and the last trip of the day

As a general practice, bus operators do not modify the starting time of the first trip of the day Ceder (2011). This requirement can be modeled by deactivating the decision variable related to the first trip of the day: $x_1 = 0$.

To avoid schedule sliding and maintain the duration of the daily operations, the last trip of the day, $|N|$, is generally requested to be dispatched before a pre-defined time of the day, $\mathcal{T}_{last}$. This results in the additional constraint:

$$a_{b_{|N|},|S|}(\boldsymbol{x}) + k_{b_{|N|},|S|}(\boldsymbol{x}) + \varphi_{b_{|N|}} \leq \mathcal{T}_{last} \tag{10}$$

4.2. Maximum dispatching headway constraint

Maximum dispatching headways are typically requested by the transit agency to ensure a minimum level of service. This results in the inequality constraints

$$(g_n + x_n) - (g_{n-1} + x_{n-1}) \leq H, \ \forall n \in N \setminus \{1\} \tag{11}$$

where H is the maximum limit of the dispatching headways of two subsequent buses. Note that the bus operators might select different values of H for peak and off-peak periods because of the different requirements about the level of service.

4.3. Objective definition

The determined trip frequencies from the frequency settings phase dictate the desired headways at bus stops. During the actual operations, the desired headways cannot be maintained because of the travel and dwell time fluctuations. Those deviations of the actual headways from their desired values are a common indicator of the service regularity (Trompet et al., 2011).

To measure the service regularity during the daily operations, we compute the square root of the average squared deviation of the actual headways from the desired/planned ones:

$$f_1(\boldsymbol{x}) = \sqrt{\frac{1}{|S|(|N|-1)} \sum_{s \in S} \sum_{n \in N \setminus \{1\}} \Big(h_{n,s}(\boldsymbol{x}) - w_s \Big)^2} \text{ (in seconds)} \tag{12}$$

where w_s is the desired/planned bus headway at any stop $s \in S$.

The objective of our study is to minimize $f_1(\boldsymbol{x})$ to improve the regularity of the service. $f_1(\boldsymbol{x})$ is selected as an indicator of the service regularity instead of the average absolute deviation from the desired headways, which can be expressed as $\frac{1}{|S|(|N|-1)} \sum_{s \in S} \sum_{n \in N \setminus \{1\}} \Big| h_{n,s}(\boldsymbol{x}) - w_s \Big|$, because it penalizes progressively the deviations from the planned headways.

Another problem objective is to ensure that our modified dispatching times do not prolong significantly the trip travel times, as it is usually the case in practice (Fu and Yang, 2002). This is an important issue because the delayed completion of bus trips has several negative effects. First, it increases the passenger travel times, and second, it delays the dispatching of future trips resulting in "schedule sliding" (Ibarra-Rojas and Rios-Solis, 2012).

In practice, transport authorities set a maximum travel time limit for the operating trips to penalize the unusually delayed ones. The travel time limit of bus trips, $\mathcal{T}_{max}$, is usually defined during the frequency settings stage. Given that $a_{n,s=|S|}(\boldsymbol{x}) - d_{n,s=1}(\boldsymbol{x})$ expresses the trip travel time of any trip $n \in N$, the term $\max\{0, \big(a_{n,s=|S|}(\boldsymbol{x}) - d_{n,s=1}(\boldsymbol{x}) - \mathcal{T}_{max}\big)\}$ expresses the excessive completion time of a trip.

This objective is selected instead of the objective of minimizing the total travel times of all passengers. The reason is that bus operators want to adhere to the scheduled trip completion times to avoid delayed future dispatches that can affect the vehicle and crew schedules. Notwithstanding the above, future studies can add the travel times of

passengers as a third objective and examine also this effect. Minimizing the excessive trip travel times of all daily trips can be expressed as:

$$f_2(\boldsymbol{x}) = \sqrt{\frac{1}{|N|}\sum_{n\in N}\Big(\max\{0, \big(a_{n,s=|S|}(\boldsymbol{x}) - d_{n,s=1}(\boldsymbol{x}) - \mathcal{T}_{max}\big)\}\Big)^2} \text{ (in seconds)} \quad (13)$$

where $f_2(\boldsymbol{x})$ is the square root of the average squared travel time prolongation of trips beyond the maximum travel time limit, $\mathcal{T}_{max}$.

By definition, $f_2(\boldsymbol{x})$ cannot be negative since $\max\{0, \big(a_{n,s=|S|}(\boldsymbol{x}) - d_{n,s=1}(\boldsymbol{x}) - \mathcal{T}_{max}\big)\} \geq 0,\ \forall n \in N$. If the travel times of all daily trips are less than the maximum imposed trip travel time limit $\mathcal{T}_{max}$, then $f_2(\boldsymbol{x})$ receives its minimum possible value ($f_2(\boldsymbol{x}) = 0$). In such case, $a_{n,s=|S|}(\boldsymbol{x}) - d_{n,s=1}(\boldsymbol{x}) \leq \mathcal{T}_{max},\ \forall n \in N$.

Remark 2: Analyzing further the total trip travel time, we get

$$a_{n,s=|S|}(\boldsymbol{x}) - d_{n,s=1}(\boldsymbol{x}) = \sum_{s\in S\setminus\{|S|\}} t_{s,\tau} + k_{n,s}(\boldsymbol{x}) \quad \text{where } \tau = \frac{|T|}{86400} d_{n,s}(\boldsymbol{x})$$

This travel time is the sum of the link travel times and the dwell times from the beginning of the trip until the last stop. Given that our decision variables control only the dispatching times of trips, we can affect the total trip travel time only indirectly.

After introducing the two objectives, it is worth noting that one should not sacrifice service regularity to ensure that all trips will be completed according to plan and vice versa. Instead, a satisfactory trade-off between those two objectives should be established. Given that our problem has two objectives, it can be formulated as a multi-objective optimization problem:

$$\underset{\boldsymbol{x}}{\text{argmin}}\big(f_1(\boldsymbol{x}), f_2(\boldsymbol{x})\big) \quad (14)$$

The multi-objective optimization problem of Eq.14 can be cast as a single-objective one with the use of the weighted sum approach. This approach introduces weight factors to establish an acceptable trade-off between the service regularity and the excessive trip travel times (see Marler and Arora (2010)). In the following, we form this single-objective function by introducing the weight factors $0 \leq \lambda_1, \lambda_2 \leq 1$ which establish the trade-off between the two objectives of the problem:

$$\begin{aligned} f(\boldsymbol{x}) := \quad & \lambda_1 f_1(\boldsymbol{x}) + \lambda_2 f_2(\boldsymbol{x}) \\ \text{s.t.} \quad & \lambda_1 + \lambda_2 = 1 \\ & 0 \leq \lambda_1, \lambda_2 \leq 1 \end{aligned} \quad (15)$$

5. Reformulation of the robust timetabling problem to an unconstrained one

Each link travel time, $t_{s,\tau}$, can take any value from the uncertainty set $\mathcal{V}_{s,\tau}$ and the hourly passenger boardings, $\beta_{s,\varrho}$, can take any value from the uncertainty set $\mathcal{U}_{s,\varrho}$. Therefore, the objective function value of Eq.15 can change based on the realizations of the link travel times and the hourly passenger boardings.

In robust optimization, we seek the dispatching time modifications, $\boldsymbol{x}$, that minimize the worst-case cost given the uncertainty sets of the link travel times and the passenger boardings as is expressed below using the minimax method (Wald (1945)):

$$\min_{\boldsymbol{x}} \max_{\boldsymbol{t},\boldsymbol{\beta}} f(\boldsymbol{x},\boldsymbol{t},\boldsymbol{\beta}) \tag{16}$$

where

$$\begin{aligned} f(\boldsymbol{x},\boldsymbol{t},\boldsymbol{\beta}) = \quad & \lambda_1 \sqrt{\frac{1}{|S|(|N|-1)} \sum_{s\in S} \sum_{n\in N\setminus\{1\}} \left(\left(a_{n,s}(\boldsymbol{x},\boldsymbol{t},\boldsymbol{\beta}) - a_{n',s}(\boldsymbol{x},\boldsymbol{t},\boldsymbol{\beta}) \right) - w_s \right)^2} \\ & + \lambda_2 \sqrt{\frac{1}{|N|} \sum_{n\in N} \left(\max\{0, \left(a_{n,s=|S|}(\boldsymbol{x},\boldsymbol{t},\boldsymbol{\beta}) - d_{n,s=1}(\boldsymbol{x},\boldsymbol{t},\boldsymbol{\beta}) - \mathcal{T}_{max} \right)\} \right)^2} \end{aligned} \tag{17}$$

and $\boldsymbol{t} = \{t_{s,\tau}\}$ and $\boldsymbol{\beta} = \{\beta_{s,\varrho}\}$ are the disturbance matrices of the link travel time and the hourly passenger boarding parameters where each element from those matrices can take values from the corresponding uncertainty set.

This allows us to cast the robust timetabling problem that considers the full set of regulatory and physical constraints as:

$$\begin{aligned} (Q): \quad \min_{\boldsymbol{x}} \max_{\boldsymbol{t},\boldsymbol{\beta}} \quad & f(\boldsymbol{x},\boldsymbol{t},\boldsymbol{\beta}) \\ \text{s.t.} \quad & a_{b_n,|S|}(\boldsymbol{x},\boldsymbol{t},\boldsymbol{\beta}) + k_{b_n,|S|}(\boldsymbol{x},\boldsymbol{t},\boldsymbol{\beta}) + \varphi_{b_n} - (g_n + x_n) \le 0, \ \forall n \in N \setminus \{1\} \\ & a_{b_{|N|},|S|}(\boldsymbol{x},\boldsymbol{t},\boldsymbol{\beta}) + k_{b_{|N|},|S|}(\boldsymbol{x},\boldsymbol{t},\boldsymbol{\beta}) + \varphi_{b_{|N|}} - \mathcal{T}_{last} \le 0 \\ & (g_n + x_n) - (g_{n-1} + x_{n-1}) \le H, \ \forall n \in N \setminus \{1\} \\ & x_1 = 0 \\ \text{where} \quad & t_{s,\tau} \in \mathcal{V}_{s,\tau}, \ \forall s \in S, \tau \in T \\ & \beta_{s,\varrho} \in \mathcal{U}_{s,\varrho}, \ \forall s \in S, \varrho \in R \\ & x_n \in Z, \ \forall n \in N \end{aligned} \tag{18}$$

Note that for different values of $\boldsymbol{x},\boldsymbol{t},\boldsymbol{\beta}$ in the above mathematical program, the values of the objective function, the arrival times of buses at stops, the number of boardings and alightings at each stop and the busloads are computed by equations 1-8, 17. The mathematical program (Q) has $2|N|-1$ inequality constraints. To evaluate the satisfaction of the inequality constraints related to the layover times, one can introduce a set of $|N||S|-1$ functions:

$$I_i(\boldsymbol{x},\boldsymbol{t},\boldsymbol{\beta}) = a_{b_n,|S|}(\boldsymbol{x},\boldsymbol{t},\boldsymbol{\beta}) + k_{b_n,|S|}(\boldsymbol{x},\boldsymbol{t},\boldsymbol{\beta}) + \varphi_{b_n} - (g_n + x_n), \ \forall i \in \{1,2,...,|N|-1\} \tag{19}$$

To evaluate the satisfaction of the schedule sliding inequality constraint:

$$I_i(\boldsymbol{x},\boldsymbol{t},\boldsymbol{\beta}) = a_{b_{|N|},|S|}(\boldsymbol{x},\boldsymbol{t},\boldsymbol{\beta}) + k_{b_{|N|},|S|}(\boldsymbol{x},\boldsymbol{t},\boldsymbol{\beta}) + \varphi_{b_{|N|}} - \mathcal{T}_{last} \text{ for } i = |N| \tag{20}$$

and the maximum headway limit inequality constraints:

$$I_i(\boldsymbol{x}, \boldsymbol{t}, \boldsymbol{\beta}) = (g_n + x_n) - (g_{n-1} + x_{n-1}) - H, \ \forall i \in \{|N|, |N|+1, ..., 2|N|-1\} \quad (21)$$

Given the uncertainty of the link travel times and the hourly passenger boardings, the solution feasibility of the mathematical program (Q) cannot be guaranteed. That is, there exists a sufficient condition under which at least one of the inequality constraints cannot be satisfied.

Lemma 5.1. *If* $\exists\ \boldsymbol{t}^0, \boldsymbol{\beta}^0$ *for which* $a_{b_{|N|},|S|}(\boldsymbol{x}, \boldsymbol{t}^0, \boldsymbol{\beta}^0) + k_{b_{|N|},|S|}(\boldsymbol{x}, \boldsymbol{t}^0, \boldsymbol{\beta}^0) + \varphi_{b_{|N|}} > \mathcal{T}_{last}$, *then the schedule sliding constraint cannot be satisfied.*

Proof. The arrival and the dwell times of trip $b_{|N|}$ at the last stop depend on the dispatching time modifications $\boldsymbol{x}$ and $\boldsymbol{t}, \boldsymbol{\beta}$. We define $Y_0(\boldsymbol{x}, \boldsymbol{t}, \boldsymbol{\beta}) := a_{b_{|N|},|S|}(\boldsymbol{x}, \boldsymbol{t}, \boldsymbol{\beta}) + k_{b_{|N|},|S|}(\boldsymbol{x}, \boldsymbol{t}, \boldsymbol{\beta})$. The function $Y_0(\boldsymbol{x}, \boldsymbol{t}, \boldsymbol{\beta})$ does not have an upper bound in $\mathbb{R}_{\geq 0}$. That is, there exists a disturbance $\boldsymbol{t}^0, \boldsymbol{\beta}^0$ such that $Y_0(\boldsymbol{x}, \boldsymbol{t}^0, \boldsymbol{\beta}^0) > \mathcal{T}_{last} - \varphi_{b_{|N|}}$, $\forall \boldsymbol{x} \in Z$ which means that program (Q) does not have a feasible solution for such $\boldsymbol{t}^0, \boldsymbol{\beta}^0$. □

Given that for some $\boldsymbol{t}^0, \boldsymbol{\beta}^0$ the mathematical program (Q) can be infeasible, we introduce an exterior point penalty function. The exterior point penalty function approximates the inequality constraints of (Q) by transforming (Q) into $(\tilde{Q})$. The exterior point penalty function of $(\tilde{Q})$ approximates the constrained optimization problem (Q) by adding penalty terms to the objective function that prescribe a high cost for each violation of the constraints (see Bertsekas (1990)).

Introducing the penalty function, $\mathcal{P}(\boldsymbol{x}, \boldsymbol{t}, \boldsymbol{\beta})$, mathematical program (Q) becomes:

$$\begin{aligned} (\tilde{Q}): \quad \min_{\boldsymbol{x}} \max_{\boldsymbol{t},\boldsymbol{\beta}} \ & \mathcal{P}(\boldsymbol{x}, \boldsymbol{t}, \boldsymbol{\beta}) := f(\boldsymbol{x}, \boldsymbol{t}, \boldsymbol{\beta}) + \sum_{i=1}^{2|N|-1} W_i (\max[0, I_i(\boldsymbol{x}, \boldsymbol{t}, \boldsymbol{\beta})])^2 \\ \text{where} \ & t_{s,\tau} \in \mathcal{V}_{s,\tau}, \ \forall s \in S, \tau \in T \\ & \beta_{s,\varrho} \in \mathcal{U}_{s,\varrho}, \ \forall s \in S, \varrho \in R \\ & x_n \in Z, \ \forall n \in N \\ & x_1 = 0 \end{aligned} \quad (22)$$

where $W_i \ggg 0 \ \forall i \in \{1, ..., |N||S| + |N|\}$ and always takes a sufficiently high value to ensure that each constraint violation is over-penalized.

The penalty function, $\mathcal{P}(\boldsymbol{x}, \boldsymbol{t}, \boldsymbol{\beta})$, is equal to the objective function, $f(\boldsymbol{x}, \boldsymbol{t}, \boldsymbol{\beta})$, if $\sum_{i=1}^{2|N|-1} W_i (\max[0, I_i(\boldsymbol{x}, \boldsymbol{t}, \boldsymbol{\beta})])^2 = 0$. This indicates that all constraints are satisfied for such values of $\boldsymbol{x}, \boldsymbol{t}, \boldsymbol{\beta}$. The term $\sum_{i=1}^{2|N|-1} W_i (\max[0, I_i(\boldsymbol{x}, \boldsymbol{t}, \boldsymbol{\beta})])^2$ is the added term to the objective function of (Q) and dictates that if a constraint $I_i(\boldsymbol{x}, \boldsymbol{t}, \boldsymbol{\beta})$ is violated (which occurs when $I_i(\boldsymbol{x}, \boldsymbol{t}, \boldsymbol{\beta}) > 0$), then $\max[0, I_i(\boldsymbol{x}, \boldsymbol{t}, \boldsymbol{\beta})] = I_i(\boldsymbol{x}, \boldsymbol{t}, \boldsymbol{\beta})$. This adds a penalty $I_i(\boldsymbol{x}, \boldsymbol{t}, \boldsymbol{\beta})$ to the objective function $f(\boldsymbol{x}, \boldsymbol{t}, \boldsymbol{\beta})$. In that case, the objective function $f(\boldsymbol{x}, \boldsymbol{t}, \boldsymbol{\beta})$ is penalized by the positive term $W_i I_i^2(\boldsymbol{x}, \boldsymbol{t}, \boldsymbol{\beta})$.

Remark 3: W_i is a weight factor for every constraint expressing the violation prominence of one constraint compared to all others. If all constraints $i \in \{1, 2, ..., 2|N|-1\}$ have the same weight factor, then they are all equally treated.

6. Solution method for the robust timetabling problem

Applying a classical exact optimization method to solve $(\tilde{Q})$ requires an exponential number of penalty function evaluations to find a globally optimal solution. For instance, the required number of penalty function evaluations with the brute-force method is $|Z|^{|N|}$ and a globally optimal solution cannot be computed in practice (i.e., for a typical bus service with 200 daily trips and a set $Z = \{-180, -120, -60, 0, +60, +120, +180\}$ seconds, the number of required penalty function evaluations is $|Z|^{|N|} = 7^{200} = 1.046184E + 169$).

Instead of using exact optimization methods, heuristic optimization algorithms, such as the ones from the area of evolutionary optimization, can be employed. Even if evolutionary optimization algorithms do not guarantee global optimality, they can be applied to attain improved solutions. In this work, we devise a genetic algorithm (GA) that incorporates sequential quadratic programming (SQP) to solve the minimax problem of $(\tilde{Q})$. This solution method searches for the dispatching times that perform best in worst-case scenarios of travel time and passenger demand disturbances.

The main stages of our proposed GA are: (1) encoding the initial population; (2) evaluating the fitness of each population member at the worst-case scenario using SQP; (3) selecting parents for offspring generation; (4) crossover; and (5) mutation.

6.1. Encoding

We initially introduce a GA population $\mathbf{P} = \{\boldsymbol{x}^1, \boldsymbol{x}^2 ..., \boldsymbol{x}^{|P|}\}$, where each population member $\boldsymbol{x}^i \in \mathbf{P}$ is an *initial solution guess* of the robust dispatching time optimization problem. The genes of each population member $\boldsymbol{x}^i = \{x_1^i, x_2^i, ..., x_{|N|}^i\}$ denote the dispatching time modification of each trip $\{1, 2, ..., |N|\}$. When initializing the population, each gene x_n^i receives a random value from the set Z.

6.2. Fitness Evaluation

Because we seek a robust timetable, the fitness of a population member $\boldsymbol{x}^i \in \mathbf{P}$ is evaluated by calculating its performance under the worst-case travel time and passenger demand disturbance. That is, the fitness $\mathcal{F}(\boldsymbol{x}^i)$ of a population member $\boldsymbol{x}^i \in \mathbf{P}$ is the optimal value function of

$$\mathcal{F}(\boldsymbol{x}^i) := \left\{ \max_{\boldsymbol{t},\boldsymbol{\beta}} \ \mathcal{P}(\boldsymbol{x}^i, \boldsymbol{t}, \boldsymbol{\beta}), \quad \text{s.t. } t_{s,\tau} \in \mathcal{V}_{s,\tau}, \ \forall s, \tau, \beta_{s,\varrho} \in \mathcal{U}_{s,\varrho}, \ \forall s, \varrho \right\} \tag{23}$$

This maximization problem can be denoted as $(\tilde{Q}_{max})$ and is a nonlinear programming problem (NLP). $(\tilde{Q}_{max})$ can be solved with numerical optimization methods for nonlinear programming, such as the sequential quadratic programming (SQP) method. In Appendix A we provide a detailed description of applying a multi-start SQP algorithm for solving the mathematical program $(\tilde{Q}_{max})$.

$(\tilde{Q}_{max})$ must be solved |P| times to return the fitness values $\mathcal{F}(\boldsymbol{x}^i)$ of each population member $\boldsymbol{x}^i \in \mathbf{P}$. One population member $\boldsymbol{x}^i \in \mathbf{P}$ is more fit for reproduction if its $\mathcal{F}(\boldsymbol{x}^i)$ value is low indicating a good performance at the worst-case scenario. Using the well-known roulette-wheel selection method Goldberg and Deb (1991), population members with better fitness have a higher probability of being selected for reproduction. In more detail, the probability of a population member $\boldsymbol{x}^j$ to be selected for reproduction is $\frac{\mathcal{F}(\boldsymbol{x}^j)}{\sum_{\boldsymbol{x}_i \in \mathbf{P}} \mathcal{F}(\boldsymbol{x}^i)}$.

6.3. Crossover and Mutation

For each pair of parents that are selected by the roulette-wheel selection method, a cross-over occurs at a randomly selected crossover point to produce two offsprings (recombination). The same process is repeated until the total number of generated offsprings is equal to the population size |P|.

In the mutation stage, a mutation can occur at any gene of an offspring allowing the exploration of new information that does not belong to the parents. That is, each gene has a very small probability of being replaced by a random value from the set Z of dispatching time deviation options.

6.4. Population Evolution and Termination

After completing the above stages, the initial population is replaced by the new generation. This procedure is repeated resulting in population evolutions $\kappa = \{1, 2, ...\}$. At each population evolution, there is an incumbent solution $\boldsymbol{x}^{\kappa}$ for which $\boldsymbol{x}^{\kappa} \leq \boldsymbol{x}^{i}, \ \forall \boldsymbol{x}^{i} \in \mathbf{P}$. The population evolutions continue until reaching a pre-determined limit of population generations without any further improvement as presented in alg.1.

Algorithm 1 Solution of the minimax problem

function MiniMax
  Set iteration $\kappa \leftarrow 1$;
  Initialize population $\mathbf{P} = \{\boldsymbol{x}^1, \boldsymbol{x}^2..., \boldsymbol{x}^{|P|}\}$;
  while the termination criterion is not achieved **do**
    Evaluate the fitness $\mathcal{F}(\boldsymbol{x}^i)$, $\forall \boldsymbol{x}^i \in \mathbf{P}$ by solving $(\tilde{Q}_{max})$ using SQP (see alg.2);
    Find the incumbent solution $\boldsymbol{x}^{\kappa} \leq \boldsymbol{x}^{i}, \ \forall \boldsymbol{x}^{i} \in \mathbf{P}$ that has the best performance in the worst-case scenario;
    Perform the crossover and mutation steps and generate a new population $\mathbf{P}$;
    Set iteration $\kappa \leftarrow \kappa + 1$;
  end while
  return the final solution $\mathbf{x}^*$
end function

7. Experimental results

7.1. Case study description

The case study is a high-frequency circular bus service in Singapore with 214 daily trips. From all daily trips, only the trips dispatched within 07:00 and 19:00 operate under a regularity-based scheme. The rest are scheduled based on punctuality and are not part of our timetabling problem. The total number of trips that operate from 07:00 until 19:00 are $|N| = 132$. The circular service covers 7.5 km and serves $|S| = 22$ bus stops with an average trip travel time of 37 minutes. The circular bus service is a feeder service covering residential blocks, schools, public amenities and connecting them to a Mass Rapid Transit (MRT) station as presented in Fig.1. In this bus line operate 12-meter single-decker buses with a seated capacity of 42 passengers and standing capacity of 33 passengers (75 passengers in total). From this line, detailed five-month AVL and APC datasets are available. The datasets contain a total number of 2,254 trips with

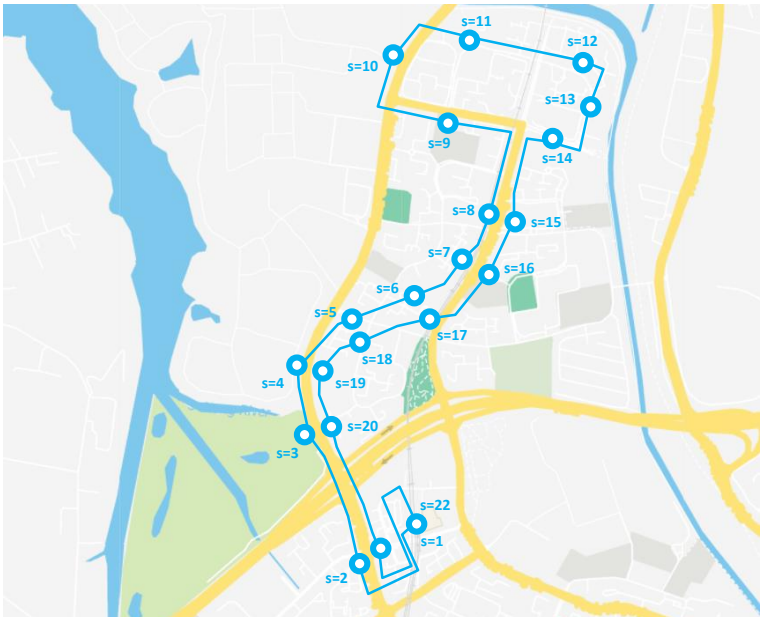

Figure 1: Bus line topology - locations of stops [map source: Google maps]

complete information regarding arrival times at stops, link travel times, boardings and alightings.

The values of the parameters for the robust timetabling problem are summarized in tables 2 and 3. $\mathcal{T}_{max}$ is derived after consultation with the bus operator and is defined as the 90% quantile of the observed total travel times. This is not restrictive though (i.e., bus operators are free to select their preferred trip travel time limits).

Table 2: Parameter values of the circular bus service

S	(bus stops)	{1,2,...,22}
$\|N\|$	(number of trips that operate under service regularity)	132
φ	(layover time)	180 sec $\rightarrow$ 3 min
p_0	(dwell time in case of no boardings/alightings)	0 sec
p_1	(required time per passenger boarding)	3 sec
p_2	(required time per passenger alighting)	1.5 sec
g_{first}	(dispatching time of the first trip)	25200 sec $\rightarrow$ 07:00
$\mathcal{T}_{last}$	(latest possible dispatching time of the last trip)	68340 sec $\rightarrow$ 18:59
$\mathcal{T}_{max}$	(maximum trip travel time limit)	2520 sec $\rightarrow$ 42 min
H	maximum allowed limit of the dispatching headways	480 sec $\rightarrow$ 8 min
$w_{s,\rho}$	(planned headway at any stop $s \in S$ in time period 07:00-10:30)	300 sec $\rightarrow$ 5 min
$w_{s,\rho}$	(planned headway at any stop $s \in S$ in time period 10:30-19:00)	360 sec $\rightarrow$ 6 min

Table 3: Originally planned trip dispatching times

N	Planned dispatching time of each trip, $g_n,\ \forall n \in N$											
{1,...,12}	7:00	7:05	7:10	7:15	7:20	7:25	7:30	7:35	7:41	7:47	7:53	7:58
{13,...,24}	8:03	8:08	8:13	8:18	8:23	8:28	8:33	8:38	8:43	8:48	8:53	8:57
{25,...,36}	9:02	9:06	9:11	9:15	9:20	9:24	9:29	9:33	9:38	9:42	9:47	9:52
{37,...,48}	9:57	10:02	10:07	10:12	10:17	10:23	10:29	10:36	10:43	10:49	10:55	11:01
{49,...,60}	11:07	11:13	11:19	11:25	11:31	11:37	11:43	11:49	11:55	12:01	12:07	12:13
{61,...,72}	12:19	12:25	12:31	12:37	12:44	12:50	12:56	13:02	13:08	13:15	13:21	13:28
{73,...,84}	13:34	13:41	13:47	13:54	14:00	14:07	14:13	14:19	14:25	14:32	14:38	14:45
{85,...,96}	14:51	14:57	15:03	15:09	15:19	15:22	15:24	15:29	15:34	15:38	15:42	15:47
{97,...,108}	15:51	16:01	16:04	16:09	16:14	16:18	16:22	16:26	16:30	16:38	16:42	16:43
{109,...,120}	16:48	16:53	16:58	17:03	17:09	17:15	17:21	17:27	17:33	17:39	17:45	17:51
{121,...,132}	17:57	18:03	18:09	18:14	18:19	18:24	18:30	18:36	18:42	18:48	18:53	18:58

Table 3 presents the originally planned dispatching times for the circular bus service from 07:00 until 19:00. The weight factors of constraints $W_i,\ \forall i \in \{1, 2, ..., 2|N| - 1\}$ are given the sufficiently high values of $10E + 5$ to ensure that the satisfaction of all problem constraints is prioritized. Later, in fig.5, we will show that the two terms f_1, f_2 of the objective function have values in the range of [0.5, 2]. Hence, a weight factor value of $10E + 5$ prioritizes the satisfaction of constraints. A practical approach to select such weight factors is to evaluate the value of the objective function by applying an initial solution guess and then select weight factor values that are significantly higher than the objective function score.

Furthermore, we apply several different weight factor values λ_1, λ_2 that dictate the trade-off between the service regularity and the excessive trip travel times to investigate the solution sensitivity to their changes. These values are presented in table 4.

Table 4: Examined pairs of weight factor values, $\lambda_1, \lambda_2 \in \mathbb{R}_{\geq 0} \mid \lambda_1 + \lambda_2 = 1$

	I	II	III	IV	V	VI
λ_1	0.8	0.66	0.5	0.09	0.05	0.025
λ_2	0.2	0.33	0.5	0.91	0.95	0.975

In Fig.2 the upper and lower limits for the link travel times are visualized as a function of the time of the day. These limits are used to form each uncertainty set, $\mathcal{V}_{s,t}$, of the link travel times where the lower and upper bounds of each set are defined as:

$$\mathcal{V}_{s,\tau} = [\mathcal{V}^{\min}_{s,\tau}, \mathcal{V}^{\max}_{s,\tau}]\ (\text{sec}) \tag{24}$$

where $\mathcal{V}^{\min}_{s,\tau} = \max\{t_s^{\text{free-flow}}, \mu_{s,\tau} - 1.96\sigma_{s,\tau}\}$ and $\mathcal{V}^{\max}_{s,\tau} = \mu_{s,\tau} + 1.96\sigma_{s,\tau}$ and $\mu_{s,\tau}, \sigma_{s,\tau}$ are the mean and standard deviation of the observed travel times of a specific link inside the time period τ. $\mu_{s,\tau} \pm 1.96\sigma_{s,\tau}$ are the 95% confidence intervals of the observed travel times and $t_s^{\text{free-flow}}$ is the free flow travel time on the specific link assuming that a bus is driving at its maximum allowed speed and is not stopped by traffic lights.

The mean and standard deviation of the link travel times are estimated using Gaussian Processes (Rasmussen and Williams, 2006). Gaussian processes assume that the underly process, in this case, the travel time at each link, is Gaussian and has a correlation function which is given by a kernel function. In our experiment we use the GPy python library (GPy, since 2012) and RBF ((Gaussian) radial basis function) or square exponential kernel.

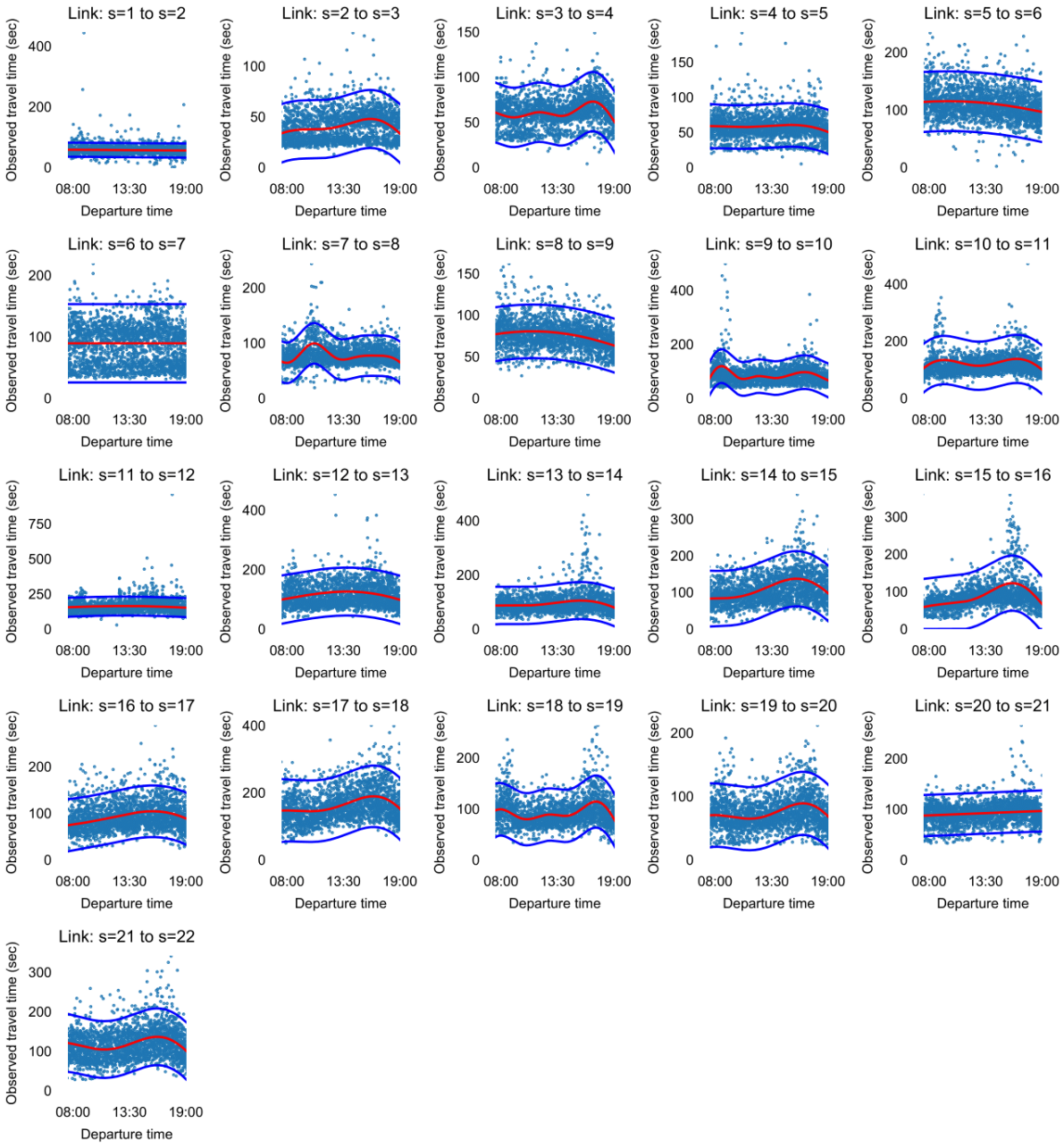

Figure 2: Upper and lower limits of the link travel times at each time of the day derived from the AVL data records

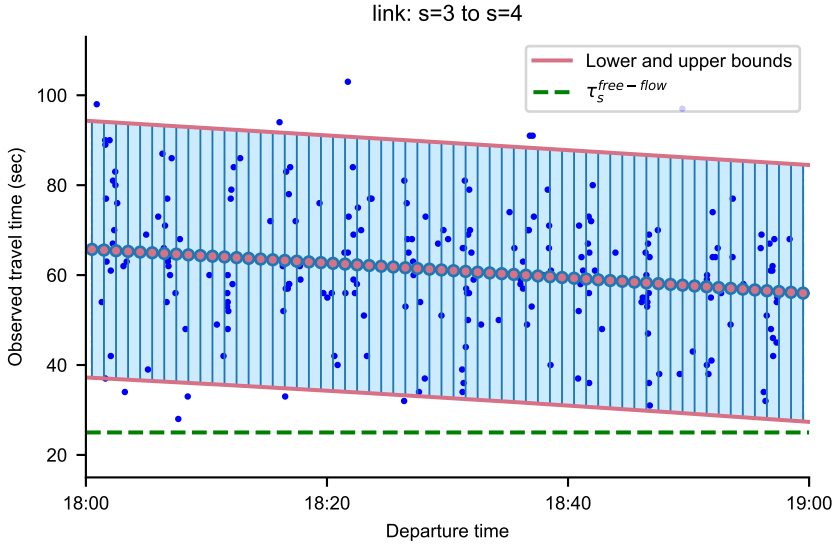

Figure 3: An example of the upper and lower limits of travel times for each 1-minute time period between 6 and 7pm. The blue lines show the computed link travel time intervals within each 1-minute period

In Fig.3, we focus explicitly in a one-hour period of a specific link from stop 3 to 4. There, we show the computed upper and lower limits of the Gaussian process approximation. In this work, we split the day into $|T| = 1440$, 1-minute time periods. Then, we derive the uncertainty set of link travel times for each time period. Therefore, each set $\mathcal{V}_{s,\tau}$ represents the uncertainty of link travel times for the minute of the day that corresponds to the respective time period of τ. In Fig.3, some values of the link travel times are outside the 95% confidence interval (outliers). Additionally, from Fig.2, 3 one can note that the mean of the link travel times varies considerably during the day.

Finally, in Fig.4 we present the lower and upper limits of the hourly passenger boardings at each stop derived from the APC data after following the same approach. The lower and upper limits are used to define the lower, $\mathcal{U}^{\min}_{s,\varrho}$, and upper bound, $\mathcal{U}^{\max}_{s,\varrho}$, for each uncertainty set $\mathcal{U}_{s,\varrho} = [\mathcal{U}^{\min}_{s,\varrho}, \mathcal{U}^{\max}_{s,\varrho}]$ at each stop $s \in S$ and hourly time period, $\varrho \in R$.

7.2. Investigating the trade-off between service regularity and excessive trip travel times

As presented in Fig.5, f_1 and f_2 receive significantly different values for different values of the weight factors λ_1, λ_2. The key observations from this analysis are:

- For $\lambda_2 \geq 0.95$, f_2 cannot be improved any further. A possible explanation is that there is a point ($\lambda \geq 0.95$) after which the travel times of some problematic trips cannot be further improved with dispatching time modifications;
- The excessive trip travel times (f_2) can be improved by 21.1% for a service regularity (f_1) sacrifice of 10.8%;
- The service regularity (f_1) can be improved by 9.7% for a sacrifice of the excessive trip travel times (f_2) of 17.4%. Note that 17.4% is the deterioration of the excessive trip travel times from 0.6075 min (when $\lambda_2 = 0.95$) to 0.7354 min (when $\lambda_2 = 0.2$);
- The service regularity (f_1) is more sensitive to changes in the weight factors λ_1, λ_2;

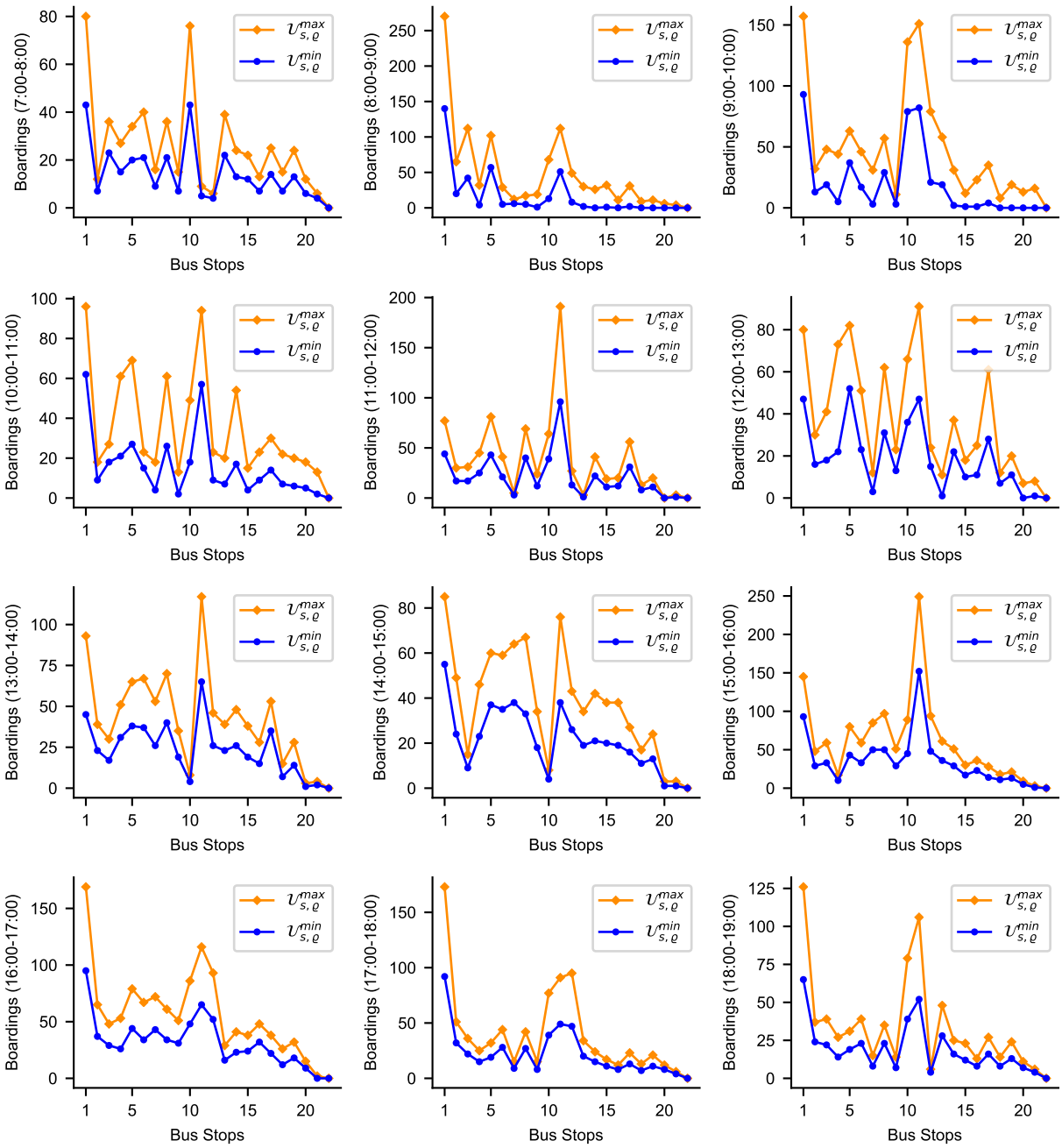

Figure 4: Upper and lower limits of the hourly passenger boardings at each stop derived from the APC data records

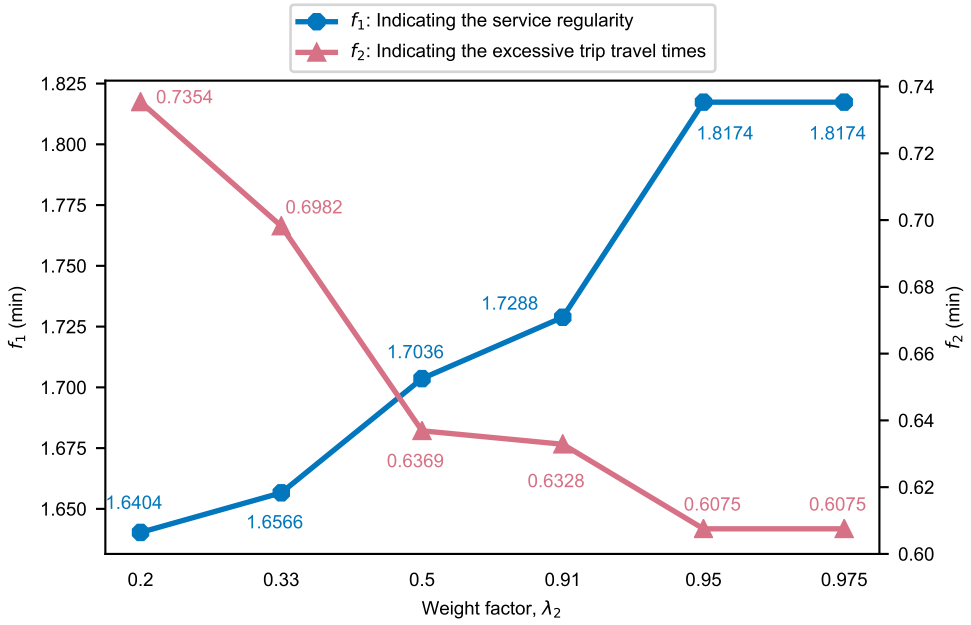

Figure 5: Plot of f_1 and f_2 for the values of the weight factors λ_1, λ_2 in table 4. Note that the horizontal axis is modified to keep the same distance among scenarios.

- Between $\lambda_2 = 0.2$ and $\lambda_2 = 0.91$ ($\lambda_1 = 0.8$ and 0.09 respectively) the service regularity, f_1, and excessive trips travel time, f_2, changes are very small denoting that this is a stable region.

The bus operator might select any weight factor pair λ_1, λ_2 to compute an optimal solution where $(\lambda_1 = 0.8, \lambda_2 = 0.8)$ places more emphasis on service regularity and $(\lambda_1 = 0.05, \lambda_2 = 0.95)$ places more emphasis on the enforcement of the trip travel time limits. If the operator has no specific preference though, the region of $0.2 \leq \lambda_2 \leq 0.91$ is the most preferable because it exhibits a balanced trade-off between the service regularity and the excessive trip travel times. Noting that $\lambda_1 = \lambda_2 = 0.5$ is the most natural choice because it places the same emphasis on the service regularity and the excessive trip travel times, we select this value to continue our analysis. We should note though that this does not prohibit the use of other values of λ_1, λ_2 if the transport operator has a specific preference.

7.3. Computation of the robust timetable

The robust timetable results after solving the problem of $(\tilde{Q})$ with alg.1 are presented in Fig.6 and the proposed robust dispatching times in table 5. The y-axis of Fig.6 presents the performance of the incumbent solution at each population evolution (iteration). In the first iteration, the maximization step easily finds a way to disrupt the current minimal solution. However, from iteration 20 the computed solutions start to exhibit some degree of robustness that is then consolidated after iteration 50. In the remaining iterations, the solution is only marginally improved.

Table 6: Assigned hyperparameter values to the eaSimple() algorithm from the Deap package for finding a new solution $\boldsymbol{x}^{\kappa}$ at each iteration

Algorithm	Hyperparameters			
eaSimple()	pop[1]=60	cxpb[2]=0.5	mutpb[3]=0.2	ngen[4]=50

[1]pop: population size
[2]cxpb: probability of pairing each individual at each generation
[3]mutpb: probability of mutating each individual at each generation
[4]ngen: number of generations to accomplish

Table 5: Robust trip dispatching times. Changes from the original dispatching times are in italics

N	Planned dispatching time of each trip, g_n, $\forall n \in N$											
{1,...,12}	7:00	7:05	7:10	7:15	7:20	7:25	7:30	7:35	7:41	7:47	7:53	7:58
{13,...,24}	8:03	8:08	8:13	8:18	8:23	8:28	8:33	*8:40*	*8:45*	*8:50*	*8:55*	*8:59*
{25,...,36}	*9:04*	*9:08*	*9:13*	*9:17*	*9:22*	*9:26*	*9:31*	*9:35*	*9:40*	*9:44*	*9:49*	*9:54*
{37,...,48}	*9:59*	*10:04*	*10:09*	*10:14*	*10:19*	*10:25*	*10:31*	*10:38*	*10:45*	*10:51*	*10:57*	*11:03*
{49,...,60}	*11:09*	*11:15*	*11:21*	*11:27*	*11:33*	*11:39*	*11:45*	*11:51*	*11:57*	*12:03*	*12:09*	*12:15*
{61,...,72}	*12:21*	*12:27*	*12:33*	*12:39*	*12:46*	*12:52*	*12:57*	*13:04*	*13:10*	*13:17*	*13:23*	13:28
{73,...,84}	*13:36*	*13:43*	*13:49*	*13:56*	*14:02*	*14:09*	*14:15*	*14:21*	*14:27*	*14:34*	*14:40*	*14:47*
{85,...,96}	*14:53*	14:57	15:03	15:09	*15:15*	15:22	15:24	15:29	15:34	15:38	15:42	15:47
{97,...,108}	15:51	*15:57*	16:04	16:09	16:14	16:18	16:22	16:26	16:30	*16:36*	*16:40*	16:43
{109,...,120}	16:48	16:53	16:58	17:03	17:09	17:15	17:21	17:27	17:33	17:39	17:45	17:51
{121,...,132}	17:57	18:03	18:09	18:14	18:19	18:24	18:30	18:36	18:42	18:48	18:53	18:58

To solve ($\tilde{Q}_{max}$) at each population evolution κ for all population members, we employ the multi-start SQP method described in alg.2. This algorithm is programmed in Python 2.7. More specifically, we deploy a multi-start SQP strategy where we generate multiple initial solution guesses. For each initial solution guess, we apply the SQP steps by using the Feasible Sequential Quadratic Programming (FSQP) method from the pyOpt Python package described in Lawrence and Tits (1996).

The GA that evolves the population is implemented with the use of the *Distributed Evolutionary Algorithms in Python* (Deap) package (Fortin et al., 2012). From this package, we use the eaSimple() algorithm with the hyperparameter values of table 6. In this study, the hyperparameter values of the GA expressed in table 6 are determined after a limited scale trial-and-error calibration. The scale of the calibration is limited because a full calibration of the hyperparameters when solving a problem instance requires to examine all possible parameter combinations (which is practically impossible given the large population size, crossover rate options, mutation rate options, and population evolution combinations). In this limited scale calibration, the GA convergence did not improve significantly for population sizes of more than 60 individuals and population evolutions of more than 50 generations. Additionally, mutation probabilities of more than 20% did not improve the solution space exploration; thus, justifying the selected hyperparameters in table 6.

After the 50$^{\text{th}}$ population evolution, the computed dispatching time solutions maintain a good performance in worst-case scenarios and the most robust solution is observed at the 72$^{\text{nd}}$ iteration for which $\mathcal{F}(\boldsymbol{x}^{\kappa=72}) = 2.34$ (expressed in min). Since the GA search cannot guarantee global optimality, the solution quality needs to be further examined. In Appendix B we analyze the solution quality in a small-scale, idealized scenario where it is possible to evaluate the performance of all solutions using as a benchmark the brute-force method that can return a globally optimal solution.

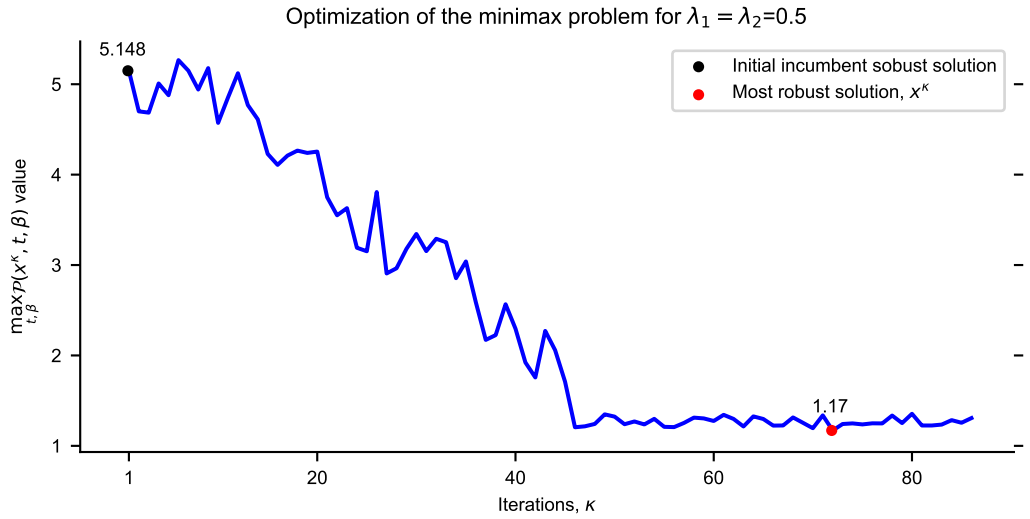

Figure 6: Iterations of alg.1 and performance of the incumbent solution at each iteration

7.4. Comparative analysis of the robust and the originally planned dispatching times in the worst-case scenario

To compute the performance of the robust timetable and the originally planned one in the worst-case scenario, we solve $(\tilde{Q}_{max})$ for the robust solution $\boldsymbol{x}^{\kappa=72}$ (worst-case scenario of the robust dispatching times) and the originally planned solution $\boldsymbol{x}^{\kappa} = \{0, ..., 0\}$. The corresponding results are presented in figures 7 and 8 respectively.

In Fig.7, we present the performance of the service regularity with the use of the originally planned and the robust dispatching times. The service regularity at each stop is calculated with the metric f_1 demonstrating a daily improvement of 9.5% when using the robust dispatching times (from 1.8832 min to 1.7036 min).

Fig.8 presents the worst-case trip travel times of the 132 trips from 07:00 until 19:00 when using the originally planned and the robust dispatching times. From Fig.8 one can observe that:

- the number of trips with travel times beyond the $\mathcal{T}_{max}$ limit of 42 min is reduced from 15 to 12 when applying the robust dispatching times;
- the overall travel time which exceeded the 42 min limit is reduced from 16.165 min to 9.588 min when applying the robust dispatching times.

It is worth noting that several of the trips from $n = 75$ to $n = 115$ exceed the maximum travel time limit and the dispatching time modifications of $\boldsymbol{x}^{\kappa=72}$ cannot satisfy this requirement. This requirement cannot be satisfied even if we place more emphasis on maintaining the trip travel times below the $\mathcal{T}_{max}$ limit. Therefore, the bus operators should be aware that, given the uncertainty of link travel times and hourly passenger boardings, there might be some problematic daily trips that cannot be completed on time.

7.5. Simulation-based validation using actual travel times and passenger boardings

In the previous analysis, we compared the performance of the originally planned dispatching times and the robust dispatching times in the respective worst-case scenarios.

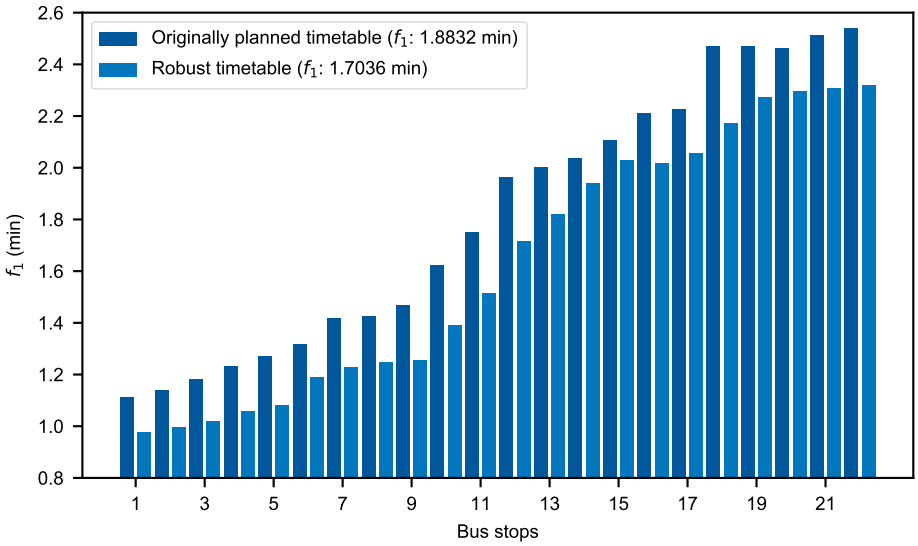

Figure 7: Worst-case performance of the service regularity at each stop with the use of the originally planned dispatching times and the robust dispatching times

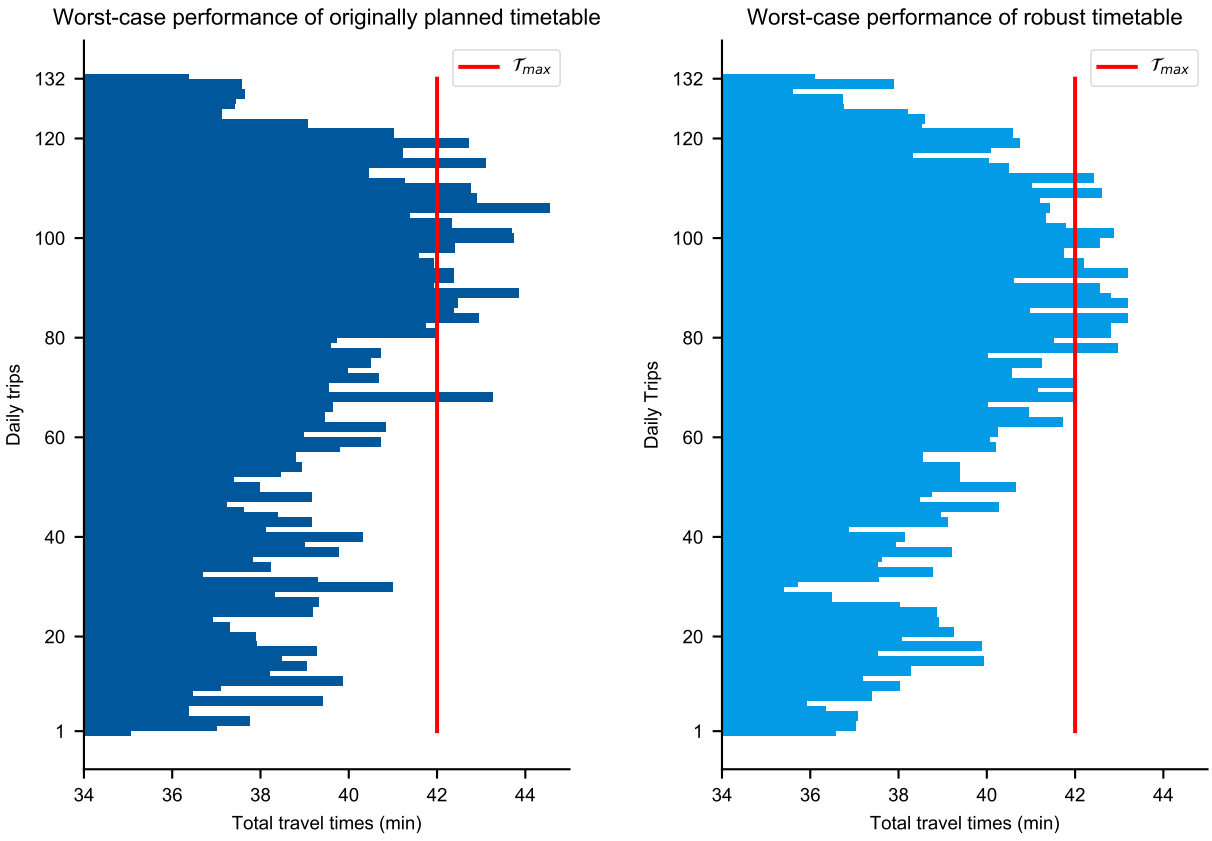

Figure 8: Worst-case trips travel times

Nevertheless, a worst-case scenario will rarely occur in practice. In this section, we sample values from the observed link travel time and hourly passenger boardings using the 5-month AVL and APC data to perform a more realistic validation.

In this simulation-based validation, we perform a large number of Monte Carlo simulations using repeated random sampling of link travel times and hourly passenger boardings from realistic data (namely, our 5-month AVL and APC datasets). In each Monte Carlo simulation, we sample the values of $\boldsymbol{t}$ and $\boldsymbol{\beta}$ representing the realizations of the link travel times and the hourly passenger boardings from the historical data. To avoid the effect of sampling bias in the validation process, we run a large number of Monte Carlo simulations, $M = 2000$.

The f_1, f_2 values are evaluated for each Monte Carlo simulation of a daily scenario when using the originally planned dispatching times and the robust ones. Note that the originally planned dispatching times correspond to the optimal dispatching times when the uncertainties of the interstation travel times and hourly passenger boardings are not taken into consideration. Note also that we compare the performance of our robust timetable(s) against the performance of the optimal timetable in the average case and not against other classic methods (i.e., the even-headway and even-load methods Ceder (2007)) because our proposed model has a profoundly different objective than such methods.

The performance of the originally planned dispatching times and the robust ones at all scenarios is summarized in Fig.9 utilizing the Tukey boxplot convention (Tukey, 1977). Following this convention (i) the first quartile, Q_1, is the middle number between the smallest number and the median of the data set, (ii) Q_2 is the median of the data set, (iii) the third quartile, Q_3, is the middle value between the median and the highest value of the data set, (iv) the minimum is the lowest datum still within 1.5 of the interquartile range (IQR) of the first quartile and, (v) the maximum is the highest datum still within 1.5 IQR of the third quartile. All other values outside the [minimum, maximum] set are outliers.

Fig.9 shows that the robust dispatching times have on average a 5.17% improved performance in terms of service regularity compared to the originally planned ones. More importantly, the maximum of the boxplot related to the service regularity is improved by 5.53% demonstrating an improved performance even at extreme scenarios. In addition, the interquartile range (IQR) of the robust dispatching times is IQR=$Q_3 - Q_1 = 1.584 - 1.498 = 0.086$ min and is slightly smaller than the observed IQR when implementing the originally planned dispatching times which is equal to 0.092 min.

From Fig.9 we notice that the service regularity of the robust timetable is consistently better than the original timetable; thus, the robust timetable is statistical dominating the originally planned one.

The right half of Fig.9 presents the values of f_2. From this, one can observe that the excessive trip travel times are improved on average by 6.87% when using the robust dispatching times. Additionally, the interquartile range shrank by 12.8% from 0.557-0.432=0.125 min to 0.109 min when applying the robust dispatching times proving that the excessive trip travel times become more stable and are closer to the mean.

Finally, we should note that defining realistic lower and upper limits for the link travel times, $[\mathcal{V}_{s,\tau}^{min}, \mathcal{V}_{s,\tau}^{max}]$, and the hourly passenger boardings, $[\mathcal{U}_{s,\rho}^{min}, \mathcal{U}_{s,\rho}^{max}]$, plays an important role in finding a robust timetable that performs well in common-case scenarios (i.e., it is not too conservative). For this reason, as one can observe from figures 2 and 4, we use

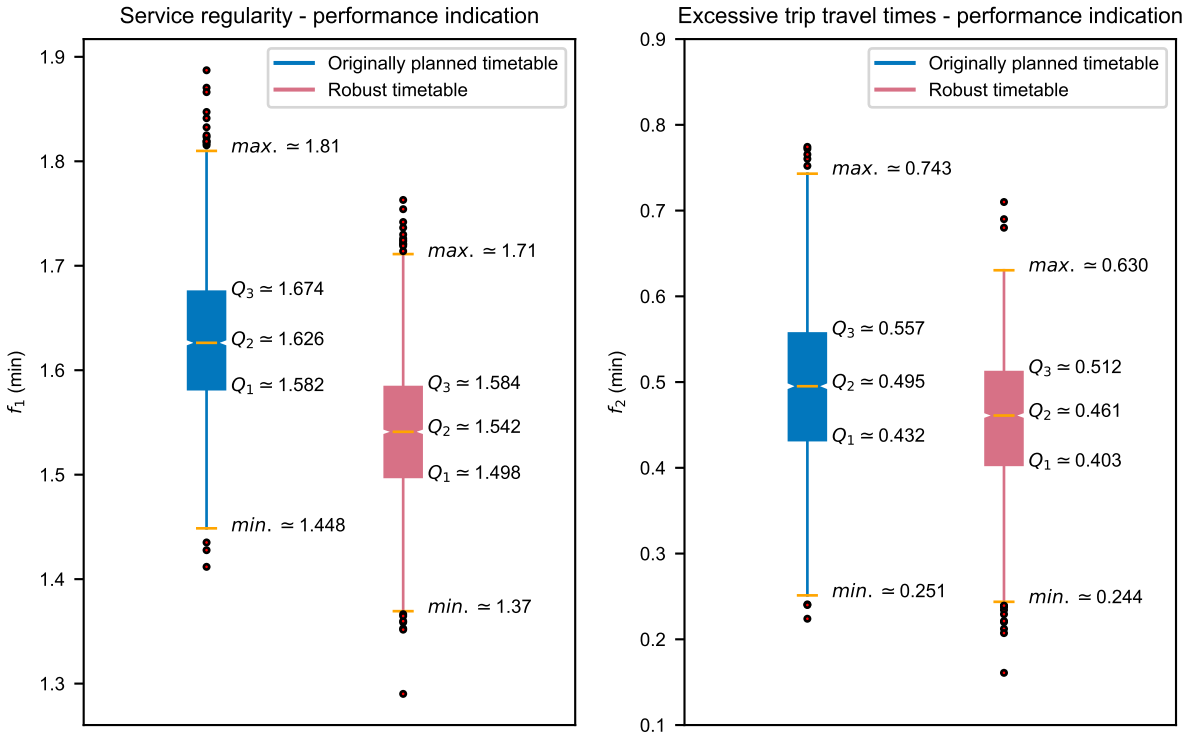

Figure 9: Validation results

Gaussian processes to derive realistic lower and upper limits and exclude outliers that have low chances to occur in practice. In this way, the robust timetable performs better in common-case scenarios while maintaining its resilience to common link travel time and hourly passenger boarding fluctuations.

To demonstrate the performance of more conservative robust timetables, we compute new timetables by increasing the limits of the link travel times and the hourly passenger boardings by 10% and 20%. Then, we present the service regularity results after applying them in the same M scenarios (table 7). Interestingly, a robust timetable which is computed considering a 20% increase in the range of the limits $[\mathcal{V}_{s,\tau}^{min}, \mathcal{V}_{s,\tau}^{max}]$ and $[\mathcal{U}_{s,\rho}^{min}, \mathcal{U}_{s,\rho}^{max}]$ exhibits a worst performance in terms of service regularity compared to the originally planned timetable (the median deteriorates by 1.66%). On the contrary, the maximum of the boxplot is reduced by 7.13% compared to the same value of the originally planned timetable. This demonstrates that service regularity will remain very close to the median value in extreme cases when using an overprotective timetable.

Table 7: Validation results - Service Regularity, f_1 (min)

Validated Timetable	min.	Q_1	median	Q_3	max.	median improvement	max. improvement
Originally Planned	1.448	1.582	1.626	1.674	1.810	N/A	N/A
Robust Timetable[1]	1.370	1.498	1.542	1.584	1.710	5.17%	5.52%
Robust Timetable[2]	1.421	1.551	1.623	1.661	1.689	0.18%	6.68%
Robust Timetable[3]	1.441	1.621	1.653	1.660	1.681	-1.66%	7.13%

[1]Calculated using the limits $[\mathcal{V}_{s,\tau}^{min}, \mathcal{V}_{s,\tau}^{max}]$ and $[\mathcal{U}_{s,\rho}^{min}, \mathcal{U}_{s,\rho}^{max}]$ depicted in figures 2 and 4
[2]Calculated using the limits $[0.90\ \mathcal{V}_{s,\tau}^{min}, 1.10\ \mathcal{V}_{s,\tau}^{max}]$ and $[0.90\ \mathcal{U}_{s,\rho}^{min}, 1.10\ \mathcal{U}_{s,\rho}^{max}]$
[3]Calculated using the limits $[0.80\ \mathcal{V}_{s,\tau}^{min}, 1.20\ \mathcal{V}_{s,\tau}^{max}]$ and $[0.80\ \mathcal{U}_{s,\rho}^{min}, 1.20\ \mathcal{U}_{s,\rho}^{max}]$

Summarizing our analysis, we enlist two weaknesses that might be instrumental in future research. First, deriving robust timetables that perform (generally) well in both common-case and worst-case scenarios requires a detailed analysis of the uncertainty sets from which the travel time and passenger boarding fluctuations can receive values. This analysis is an added task that is not required in deterministic methods. Second, the solution of a robust timetable problem with discrete decision variables requires using heuristics that do not guarantee the computation of a globally optimal solution.

7.6. Comparison of robust and stochastic optimization solutions

In the previous sub-section we compared the performances of the originally planned timetable based on nominal conditions and the robust optimization timetable in $M = 2000$ daily scenarios demonstrating a potential improvement of 5.17% in terms of service regularity. Another valuable test is the comparison of the robust timetable against a timetable computed with stochastic optimization. Stochastic optimization is an alternative approach that can optimize a timetable in the presence of uncertainty. Stochastic optimization uses random variables of known probability distributions in the optimization process and seeks a solution that minimizes the expected performance of the objective function in the presence such random variables (Shapiro et al., 2009; Naumann et al., 2011).

In this sub-section, we compare the performance of the robust timetable and the stochastic optimization timetable in 2000 daily scenarios to investigate the similarities and differences of the two approaches. To compute a timetable based on stochastic optimization, we use the mean $\mu_{s,\tau}$ and variance $\sigma^2_{s,\tau}$ of the observed travel times from the historical, 5-month AVL data presented in Fig.2. In addition, we use the mean $\tilde{\mu}_{s,\varrho}$ and variance $\tilde{\sigma}^2_{s,\varrho}$ of the hourly passenger boardings at each stop s and hour ϱ as they were derived from the historical APC data (Fig.4). In stochastic optimization, the travel time from stop s to stop $s+1$ at time τ is a random variable $t_{s,\tau}$ that follows some probability distribution $t_{s,\tau} \sim \mathcal{X}(\mu_{s,\tau}, \sigma^2_{s,\tau})$. Similarly, the hourly passenger boardings follow some probability distribution $\beta_{s,\varrho} \sim \tilde{\mathcal{X}}(\tilde{\mu}_{s,\varrho}, \tilde{\sigma}^2_{s,\varrho})$.

In accordance with previous works (Dessouky et al., 2003; Xuan et al., 2011; Hans et al., 2015a), the normal distribution is selected as the probability distribution of the link travel times, $t_{s,\tau} \sim \mathcal{N}(\mu_{s,\tau}, \sigma^2_{s,\tau})$, where $t_{s,\tau} \geq t_s^{\text{free-flow}}$ and $t_s^{\text{free-flow}}$ is the lowest possible travel time under free flow conditions. Similarly, the hourly passenger boardings $\beta_{s,\rho} \sim \tilde{\mathcal{N}}(\tilde{\mu}_{s,\rho}, \tilde{\sigma}^2_{s,\varrho})$ where $\beta_{s,\varrho} \geq 0,\ \forall s \in S, \varrho \in R$ because passenger boardings cannot receive a negative value.

Using the probability distributions, the robust optimization program $\tilde{Q}$ is transformed into a stochastic optimization one:

$$
\begin{aligned}
(\hat{Q}): \quad & \min_{\boldsymbol{x}} \ \mathbb{E}[\mathcal{P}(\boldsymbol{x}, \boldsymbol{t}, \boldsymbol{\beta})] \\
\text{where} \quad & t'_{s,\tau} \sim \mathcal{N}(\mu_{s,\tau}, \sigma^2_{s,\tau}),\ \forall s \in S, \tau \in T \\
& t_{s,\tau} = \max\{t_s^{\text{free-flow}}, t'_{s,\tau}\},\ \forall s \in S, \tau \in T \\
& \beta'_{s,\varrho} \sim \tilde{\mathcal{N}}(\tilde{\mu}_{s,\rho}, \tilde{\sigma}^2_{s,\varrho}),\ \forall s \in S, \varrho \in R \\
& \beta_{s,\varrho} = \max\{0, \beta'_{s,\varrho}\},\ \forall s \in S, \varrho \in R \\
& x_n \in Z,\ \forall n \in N \\
& x_1 = 0
\end{aligned}
\tag{25}
$$

The stochastic optimization program ($\hat{Q}$) can be solved with iterative approximation methods that try to minimize the expected value $\mathbb{E}[\mathcal{P}(\boldsymbol{x}, \boldsymbol{t}, \boldsymbol{\beta})]$. An example is the Sample Average Approximation (SAA) method (Robinson, 1996) that uses a combination of sampling and deterministic optimization to provide an approximate solution of ($\hat{Q}$).

SAA tries to approximate the value of $\mathbb{E}[\mathcal{P}(\boldsymbol{x}, \boldsymbol{t}, \boldsymbol{\beta})]$ with the use of Monte Carlo sampling. In this pursue, the problem is optimized considering a very large number of realizations $(t_{s,\tau})_{l=1}^{r}$ and $(\beta_{s,\varrho})_{l=1}^{r}$. Program $\hat{Q}$ is solved deterministically for the respective realizations $\boldsymbol{t}^l = (t_{s,\tau})_l$ and $\boldsymbol{\beta}^l = (\beta_{s,\varrho})_l$. SAA returns an approximate stochastic optimization solution $\boldsymbol{x}^*$ that is close to the solution of $\hat{Q}$ if the sample size r is very large. To obtain the stochastic optimization solution with SAA, the following program is solved:

$$
\begin{aligned}
\min_{\boldsymbol{x}} \quad & \frac{1}{r}\sum_{l=1}^{r} \mathcal{P}(\boldsymbol{x}, \boldsymbol{t}^l, \boldsymbol{\beta}^l) \\
\text{where} \quad & (t'_{s,\tau})_l \sim \mathcal{N}(\mu_{s,\tau}, \sigma^2_{s,\tau}), \ \forall s \in S, \tau \in T, l \in \{1, 2, ..., r\} \\
& (t_{s,\tau})_l = \max\{t_s^{\text{free-flow}}, (t'_{s,\tau})_l\}, \ \forall s \in S, \tau \in T, l \in \{1, 2, ..., r\} \\
& (\beta'_{s,\varrho})_l \sim \tilde{\mathcal{N}}(\tilde{\mu}_{s,\rho}, \tilde{\sigma}^2_{s,\varrho}), \ \forall s \in S, \varrho \in R, l \in \{1, 2, ..., r\} \\
& (\beta_{s,\varrho})_l = \max\{0, (\beta'_{s,\varrho})_l\}, \ \forall s \in S, \varrho \in R, l \in \{1, 2, ..., r\} \\
& x_n \in Z, \ \forall n \in N \\
& x_1 = 0
\end{aligned}
\tag{26}
$$

The obtained timetable from the SAA solution is compared against the robust timetable when they are both applied to the same $M = 2000$ daily scenarios derived from real data. The results in terms of service regularity are summarized in Fig.10 utilizing the Tukey boxplot convention.

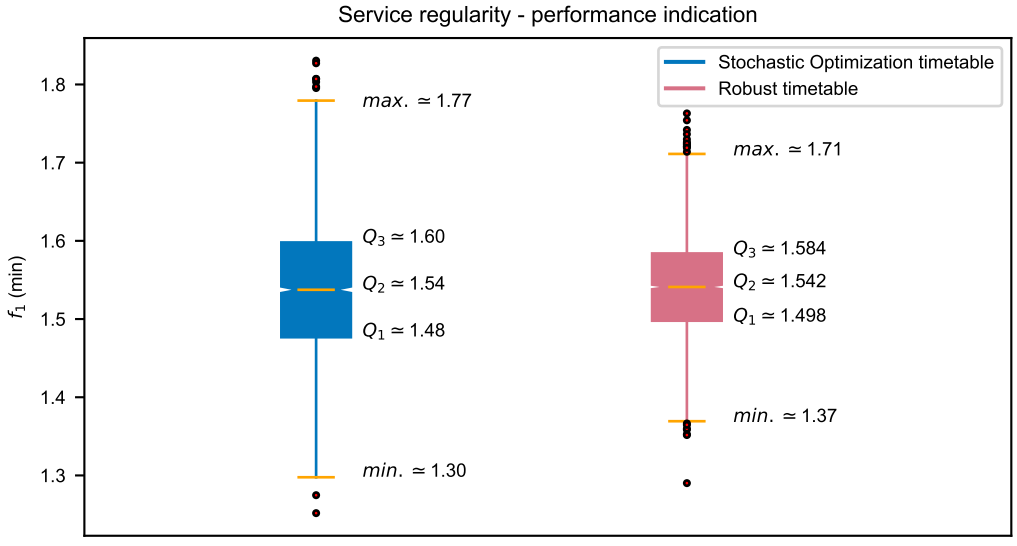

Figure 10: Validation results when comparing the robust timetable against the stochastic optimization one

On average, the stochastic optimization timetable exhibits a similar performance as the robust timetable ($Q_2 \simeq 1.54$). Nevertheless, in many daily scenarios where the travel times

and hourly passenger boardings exhibit a mild variation from their expected values, the stochastic optimization timetable is performing better. For instance, the service regularity when using a stochastic timetable can fall even below 1.3 minutes when the travel time and hourly passenger boarding realizations of a daily scenario are close to their expected values. In contrary, in daily scenarios with significant travel time and hourly passenger boarding disruptions, the stochastic optimization timetable underperforms (max value of 1.77 min), and the robust timetable is preferable (max 1.71 min). The reason behind this is that the stochastic optimization timetable is unsatisfactory if the realized travel times and boardings are at the low-probability regions of the respective probability distributions.

All in all, the robust and the stochastic optimization timetables exhibit a similar performance (on average) when applied in the 2000 daily scenarios. The main difference is that the robust timetable performs better in worst-case scenarios, whereas the stochastic optimization timetable exhibits a superior performance in the normal cases with mild disruptions. This indicates that selecting a robust timetable instead of a stochastic optimization one is a delicate task and depends on the observed variability of the travel times and passenger demand from day to day. Thus, transport operators should be aware of that and examine the trade-off between performance improvement in the normal cases and in worst-case scenarios given the variability of their daily services.

8. Concluding remarks and managerial implications

In this work, we introduced a bus movement mathematical model that can cope with travel time and passenger boarding uncertainty in the pursuit of developing robust timetables. The performance of the robust timetable for the worst-case link travel time and hourly passenger boarding scenario in a circular bus line in Singapore demonstrated an improvement potential of 9.5% in terms of service regularity.

The performance of the robust timetable against the optimal timetable in the average case was validated using AVL and APC data from a 5-month period. In the validation, the average service regularity improved by 5.17%. Additionally, the excessive trip travel times improved by 6.87% demonstrating the potential of improving both the service regularity and the excessive trip travel times by modifying the dispatching times of the daily trips.

The results of this research suggest some important managerial implications for bus operators. One managerial implication is possible changes at the crew schedules. Although the pre-determined frequencies remain unchanged when adopting a robust timetable, the dispatching times of trips should be modified. As presented in table 5, the requested dispatching time modifications when switching from an originally planned to a robust timetable are small. Therefore, switching from originally planned to robust timetables is expected to have a minor effect to the pre-determined crew schedules.

Another managerial implication is that practitioners need to thoroughly consider the bounds of the uncertainty sets for travel times and passenger boardings when developing a robust timetable. As shown in table 7, if practitioners plan timetables that are robust to significant disturbances which rarely appear in practice, the timetables will exhibit inferior performance in common case scenarios (and vice versa).

Although this study demonstrated the potential benefits of adopting robust timetables, the findings should be viewed in light of some limitations. First, our robust timetables are planned for high-frequency services where it is safe to assume that passengers cannot coordinate their arrivals at stops with the arrivals of buses (Welding, 1957; Randall et al.,

2007). Second, the determined frequencies that precede the timetabling stage should be such that passenger demand is met even at the maximum load section. If this is not the case, overcrowding issues might alter the improvement potential of robust timetables. Finally, the bus drivers should be willing to operate according to the new dispatching times of the robust timetables. If bus drivers do not conform to the recommended dispatching times, the potential benefit might shrink.

In future research, the proposed robust timetabling approach can be applied to other problems such as the timetable synchronization problem which is typically solved with deterministic approaches (Wu et al., 2015). Moreover, our approach can be applied to the optimal slack time problem. The latter can be instrumental in the application of real-time control measures such as bus holdings and stop-skipping without resulting in schedule sliding or affecting the vehicle and crew schedules.

REFERENCES

Adamski, A., Turnau, A., 1998. Simulation support tool for real-time dispatching control in public transport. Transportation Research Part A: Policy and Practice 32 (2), 73–87.

Andersson, P.-Å., Scalia-Tomba, G.-P., 1981. A mathematical model of an urban bus route. Transportation Research Part B: Methodological 15 (4), 249–266.

Ávila-Torres, P., López-Irarragorri, F., Caballero, R., Ríos-Solís, Y., 2017. The multimodal and multiperiod urban transportation integrated timetable construction problem with demand uncertainty. Journal of Industrial & Management Optimization, 29–42.

Bertini, R. L., El-Geneidy, A. M., 2004. Modeling transit trip time using archived bus dispatch system data. Journal of transportation engineering 130 (1), 56–67.

Bertsekas, D. P., 1990. Nonlinear programming, second edition Edition. Athena Scientific, Belmont, Massachusetts.

Calabrese, F., Ferrari, L., Blondel, V. D., 2015. Urban sensing using mobile phone network data: a survey of research. Acm computing surveys (csur) 47 (2), 25.

Ceder, A., 2007. Public transit planning and operation: Modeling, practice and behavior. CRC press.

Ceder, A., Golany, B., Tal, O., 2001. Creating bus timetables with maximal synchronization. Transportation Research Part A: Policy and Practice 35 (10), 913–928.

Ceder, A. A., 2011. Optimal multi-vehicle type transit timetabling and vehicle scheduling. Procedia-Social and Behavioral Sciences 20, 19–30.

Ceder, A. A., Hassold, S., Dano, B., 2013. Approaching even-load and even-headway transit timetables using different bus sizes. Public Transport 5 (3), 193–217.

Cevallos, F., Zhao, F., 2006. Minimizing transfer times in public transit network with genetic algorithm. Transportation Research Record: Journal of the Transportation Research Board (1971), 74–79.

Chaniotakis, E., Antoniou, C., 2015. Use of geotagged social media in urban settings: Empirical evidence on its potential from twitter. In: Intelligent Transportation Systems (ITSC), 2015 IEEE 18th International Conference on. IEEE, pp. 214–219.

Chen, X., Hellinga, B., Chang, C., Fu, L., 2015. Optimization of headways with stop-skipping control: a case study of bus rapid transit system. Journal of advanced transportation 49 (3), 385–401.

Daduna, J. R., Voß, S., 1995. Practical experiences in schedule synchronization. In: Computer-Aided Transit Scheduling. Springer, pp. 39–55.

Daganzo, C. F., 2009. A headway-based approach to eliminate bus bunching: Systematic analysis and comparisons. Transportation Research Part B: Methodological 43 (10), 913–921.

Dessouky, M., Hall, R., Zhang, L., Singh, A., 2003. Real-time control of buses for schedule coordination at a terminal. Transportation Research Part A: Policy and Practice 37 (2), 145–164.

Dugas, C., Bengio, Y., Bélisle, F., Nadeau, C., Garcia, R., 2001. Incorporating second-order functional knowledge for better option pricing, 472–478.

Eranki, A., 2004. A model to create bus timetables to attain maximum synchronization considering waiting times at transfer stops.

Farahani, R. Z., Miandoabchi, E., Szeto, W. Y., Rashidi, H., 2013. A review of urban transportation network design problems. European Journal of Operational Research 229 (2), 281–302.

Fortin, F.-A., De Rainville, F.-M., Gardner, M.-A., Parizeau, M., Gagné, C., jul 2012. DEAP: Evolutionary algorithms made easy. Journal of Machine Learning Research 13, 2171–2175.

Fu, L., Yang, X., 2002. Design and implementation of bus-holding control strategies with real-time information. Transportation Research Record: Journal of the Transportation Research Board (1791), 6–12.

Furth, P. G., Wilson, N. H., 1981. Setting frequencies on bus routes: Theory and practice. Transportation Research Record 818 (1981), 1–7.

Gallo, G., Miele, F. D., 2001. Dispatching buses in parking depots. Transportation Science 35 (3), 322–330.

Gkiotsalitis, K., 2019. Robust stop-skipping at the tactical planning stage with evolutionary optimization. Transportation research record 2673 (3), 611–623.

Gkiotsalitis, K., Cats, O., 2018. Reliable frequency determination: Incorporating information on service uncertainty when setting dispatching headways. Transportation Research Part C: Emerging Technologies 88, 187–207.

Gkiotsalitis, K., Cats, O., 2019. Multi-constrained bus holding control in time windows with branch and bound and alternating minimization. Transportmetrica B: Transport Dynamics 7 (1), 1258–1285.

Gkiotsalitis, K., Kumar, R., 2018. Bus operations scheduling subject to resource constraints using evolutionary optimization. Informatics 5 (1).

Gkiotsalitis, K., Maslekar, N., 2018a. Multiconstrained timetable optimization and performance evaluation in the presence of travel time noise. Journal of Transportation Engineering, Part A: Systems 144 (9).

Gkiotsalitis, K., Maslekar, N., 2018b. Towards transfer synchronization of regularity-based bus operations with sequential hill-climbing. Public transport, 1–27.

Gkiotsalitis, K., Stathopoulos, A., 2015. A utility-maximization model for retrieving users willingness to travel for participating in activities from big-data. Transportation Research Part C: Emerging Technologies 58, 265–277.

Gkiotsalitis, K., Stathopoulos, A., 2016. Joint leisure travel optimization with user-generated data via perceived utility maximization. Transportation Research Part C: Emerging Technologies 68, 532–548.

Gkiotsalitis, K., Wu, Z., Cats, O., 2019. A cost-minimization model for bus fleet allocation featuring the tactical generation of short-turning and interlining options. Transportation Research Part C: Emerging Technologies 98, 14–36.

Goldberg, D. E., Deb, K., 1991. A comparative analysis of selection schemes used in genetic algorithms. In: Foundations of genetic algorithms. Vol. 1. Elsevier, pp. 69–93.

GPy, since 2012. GPy: A Gaussian processes framework in python. http://sheffieldml.github.io/GPy/, [Online; accessed 15-March-2018].

Grant-Muller, S. M., Gal-Tzur, A., Minkov, E., Nocera, S., Kuflik, T., Shoor, I., 2014. Enhancing transport data collection through social media sources: methods, challenges and opportunities for textual data. IET Intelligent Transport Systems 9 (4), 407–417.

Guenthner, R. P., Sinha, K. C., 1983. Modeling bus delays due to passenger boardings and alightings. Transportation Research Record (915).

Guo, X., Wu, J., Zhou, J., Yang, X., Wu, D., Gao, Z., 2018. First-train timing synchronisation using multi-objective optimisation in urban transit networks. International Journal of Production Research, 1–16.
URL https://doi.org/10.1080/00207543.2018.1542177

Hans, E., Chiabaut, N., Leclercq, L., 2015a. Investigating the irregularity of bus routes: highlighting how underlying assumptions of bus models impact the regularity results. Journal of Advanced Transportation 49 (3), 358–370.

Hans, E., Chiabaut, N., Leclercq, L., Bertini, R. L., 2015b. Real-time bus route state forecasting using particle filter and mesoscopic modeling. Transportation Research Part C: Emerging Technologies 61, 121–140.

Hernández, D., Muñoz, J. C., Giesen, R., Delgado, F., 2015. Analysis of real-time control strategies in a corridor with multiple bus services. Transportation Research Part B: Methodological 78, 83–105.

Hickman, M. D., 2001. An analytic stochastic model for the transit vehicle holding problem. Transportation Science 35 (3), 215–237.

Ibarra-Rojas, O., Delgado, F., Giesen, R., Muñoz, J., 2015. Planning, operation, and control of bus transport systems: A literature review. Transportation Research Part B: Methodological 77, 38–75.

Ibarra-Rojas, O. J., Rios-Solis, Y. A., 2012. Synchronization of bus timetabling. Transportation Research Part B: Methodological 46 (5), 599–614.

Jansson, K., Pyddoke, R., 2010. Quality incentives and quality outcomes in procured public transport–case study stockholm. Research in Transportation Economics 29 (1), 11–18.

Kang, L., Zhu, X., Sun, H., Wu, J., Gao, Z., Hu, B., 2019. Last train timetabling optimization and bus bridging service management in urban railway transit networks. Omega 84, 31–44.

Kraft, W. H., Bergen, T. F., 1974. Evaluation of passenger service times for street transit systems. Transportation Research Record (505).

Lawrence, C. T., Tits, A. L., 1996. Nonlinear equality constraints in feasible sequential quadratic programming. Optimization Methods and Software 6 (4), 265–282.

Leong, W., Goh, K., Hess, S., Murphy, P., 2016. Improving bus service reliability: The singapore experience. Research in Transportation Economics 59, 40–49.

Levinson, H. S., 1983. Analyzing transit travel time performance. Transportation Research Record (915).

Liu, Z., Yan, Y., Qu, X., Zhang, Y., 2013. Bus stop-skipping scheme with random travel time. Transportation Research Part C: Emerging Technologies 35, 46–56.

Marler, R. T., Arora, J. S., 2010. The weighted sum method for multi-objective optimization: new insights. Structural and multidisciplinary optimization 41 (6), 853–862.

Marzat, J., Walter, E., Piet-Lahanier, H., 2016. A new expected-improvement algorithm for continuous minimax optimization. Journal of Global Optimization 64 (4), 785–802.

Murty, K. G., Yu, F.-T., 1988. Linear complementarity, linear and nonlinear programming. Vol. 3. Heldermann Berlin.

Naumann, M., Suhl, L., Kramkowski, S., 2011. A stochastic programming approach for robust vehicle scheduling in public bus transport. Procedia - Social and Behavioral Sciences 20, 826–835.
URL https://linkinghub.elsevier.com/retrieve/pii/S1877042811014716

Newell, G. F., 1974. Control of pairing of vehicles on a public transportation route, two vehicles, one control point. Transportation Science 8 (3), 248–264.

Niu, H., Tian, X., Zhou, X., 2015a. Demand-driven train schedule synchronization for high-speed rail lines. IEEE Transactions on Intelligent Transportation Systems 16 (5), 2642–2652.

Niu, H., Zhou, X., Gao, R., 2015b. Train scheduling for minimizing passenger waiting time with time-dependent demand and skip-stop patterns: Nonlinear integer programming models with linear constraints. Transportation Research Part B: Methodological 76, 117–135.

Pangilinan, C., Wilson, N., Moore, A., 2008. Bus supervision deployment strategies and use of real-time automatic vehicle location for improved bus service reliability. Transportation Research Record: Journal of the Transportation Research Board (2063), 28–33.

Peeters, L., Kroon, L., 2001. A cycle based optimization model for the cyclic railway timetabling problem. Computer-aided scheduling of public transport, 275–296.

Randall, E. R., Condry, B. J., Trompet, M., Campus, S. K., 2007. International bus system benchmarking: Performance measurement development, challenges, and lessons learned. In: Transportation Research Board 86th Annual Meeting, 21st-25th january.

Rasmussen, C. E., Williams, C. K., 2006. Gaussian processes for machine learning. 2006. The MIT Press, Cambridge, MA, USA 38, 715–719.

Robinson, S. M., 1996. Analysis of sample-path optimization. Mathematics of Operations Research 21 (3), 513–528.

Sels, P., Dewilde, T., Cattrysse, D., Vansteenwegen, P., 2016. Reducing the passenger travel time in practice by the automated construction of a robust railway timetable. Transportation Research Part B: Methodological 84, 124–156.

Shafahi, Y., Khani, A., 2010. A practical model for transfer optimization in a transit network: Model formulations and solutions. Transportation Research Part A: Policy and Practice 44 (6), 377–389.

Shapiro, A., Dentcheva, D., Ruszczyski, A., Jan. 2009. Lectures on Stochastic Programming: Modeling and Theory. Society for Industrial and Applied Mathematics.
URL http://epubs.siam.org/doi/book/10.1137/1.9780898718751

Sun, A., Hickman, M., 2005. The real–time stop–skipping problem. Journal of Intelligent Transportation Systems 9 (2), 91–109.

Sun, D. J., Xu, Y., Peng, Z.-R., 2015. Timetable optimization for single bus line based on hybrid vehicle size model. Journal of Traffic and Transportation Engineering (English Edition) 2 (3), 179–186.

Sun, H., Wu, J., Ma, H., Yang, X., Gao, Z., 2018. A bi-objective timetable optimization model for urban rail transit based on the time-dependent passenger volume. IEEE Transactions on Intelligent Transportation Systems.

Toole, J. L., Colak, S., Sturt, B., Alexander, L. P., Evsukoff, A., González, M. C., 2015. The path most traveled: Travel demand estimation using big data resources. Transportation Research Part C: Emerging Technologies 58, 162–177.

Trompet, M., Liu, X., Graham, D., 2011. Development of key performance indicator to compare regularity of service between urban bus operators. Transportation Research Record: Journal of the Transportation Research Board (2216), 33–41.

Tukey, J. W., 1977. Exploratory data analysis. Vol. 2. Reading, Mass.

Uniman, D., Attanucci, J., Mishalani, R., Wilson, N., 2010. Service reliability measurement using automated fare card data: Application to the london underground. Transportation Research Record: Journal of the Transportation Research Board (2143), 92–99.

Vuchic, V. R., 2017. Urban transit: operations, planning, and economics. John Wiley & Sons.

Wald, A., 1945. Statistical decision functions which minimize the maximum risk. Annals of Mathematics, 265–280.

Wang, Y., Zhang, D., Hu, L., Yang, Y., Lee, L. H., 2017. A data-driven and optimal bus scheduling model with time-dependent traffic and demand. IEEE Transactions on Intelligent Transportation Systems 18 (9), 2443–2452.

Wei, M., Sun, B., 2017. Bi-level programming model for multi-modal regional bus timetable and vehicle dispatch with stochastic travel time. Cluster Computing 20 (1), 401–411.

Welding, P., 1957. The instability of a close-interval service. Journal of the operational research society 8 (3), 133–142.

Wu, W., Liu, R., Jin, W., 2017. Modelling bus bunching and holding control with vehicle overtaking and distributed passenger boarding behaviour. Transportation Research Part B: Methodological 104, 175–197.

Wu, Y., Tang, J., Yu, Y., Pan, Z., 2015. A stochastic optimization model for transit network timetable design to mitigate the randomness of traveling time by adding slack time. Transportation Research Part C: Emerging Technologies 52, 15–31.

Xuan, Y., Argote, J., Daganzo, C. F., 2011. Dynamic bus holding strategies for schedule reliability: Optimal linear control and performance analysis. Transportation Research Part B: Methodological 45 (10), 1831–1845.

Yan, S., Chi, C.-J., Tang, C.-H., 2006. Inter-city bus routing and timetable setting under stochastic demands. Transportation Research Part A: Policy and Practice 40 (7), 572–586.

Yang, S., Wu, J., Sun, H., Yang, X., Gao, Z., Chen, A., 2017. Bi-objective nonlinear programming with minimum energy consumption and passenger waiting time for metro systems, based on the real-world smart-card data. Transportmetrica B: Transport Dynamics, 1–18.

Yin, H., Wu, J., Sun, H., Kang, L., Liu, R., 2018. Optimizing last trains timetable in the urban rail network: social welfare and synchronization. Transportmetrica B: Transport Dynamics, 1–25.

Yu, H., Ma, H., Du, H., Li, X., Xiao, R., Du, Y., 2017. Bus scheduling timetable optimization based on hybrid bus sizes. In: UK Workshop on Computational Intelligence. Springer, pp. 337–348.

Yu, Y., Ye, Z., Wang, C., 2015. Study of bus stop skipping scheme based on modified cellular genetic algorithm. In: CICTP 2015. pp. 2397–2409.

Zhang, H., Zhao, S., Cao, Y., Liu, H., Liang, S., 2017. Real-time integrated limited-stop and short-turning bus control with stochastic travel time. Journal of Advanced Transportation 2017.

Zhao, F., Zeng, X., 2008. Optimization of transit route network, vehicle headways and timetables for large-scale transit networks. European Journal of Operational Research 186 (2), 841–855.

Zhao, J., Dessouky, M., Bukkapatnam, S., 2006. Optimal slack time for schedule-based transit operations. Transportation Science 40 (4), 529–539.

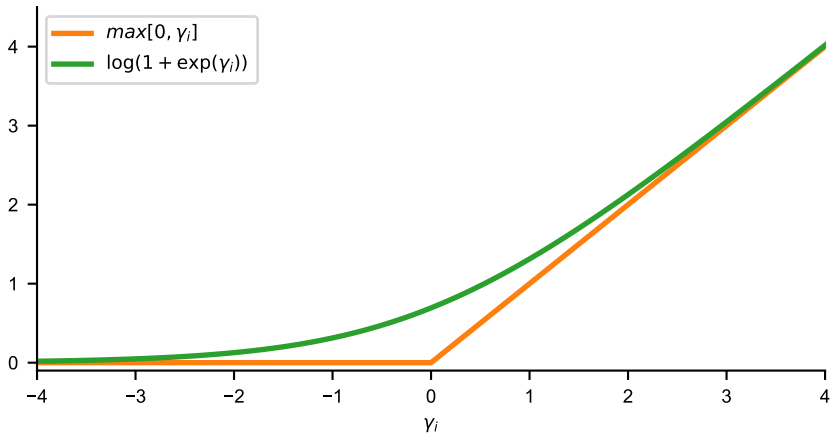

Figure A.11: Comparison between $\max[0, \gamma_i]$ and $\text{softplus}(\gamma_i)$ for $\gamma_i \in [-4, +4]$

Appendix A. Solving $(\tilde{Q}_{max})$ with multi-start sequential quadratic programming

SQP converges to a locally optimal solution for a given initial solution guess. Hence, one should compute several locally optimal solutions with the use of SQP for increasing the probability that one of the locally optimal solutions is also a globally optimal one. Eq.23, which is maximized by the multi-start SQP approach, contains several terms of the form $\max[0, \gamma_i]$ where γ_i can be any inequality constraint $I_i(\boldsymbol{x}^\kappa, \boldsymbol{t}, \boldsymbol{\beta})$. Such functions of the form $\max[0, \gamma_i]$ are known as activation functions and, in practical implementations, they can be approximated by smooth functions for facilitating the use of SQP. One of the most well-known smooth approximation functions of $\max[0, \gamma_i]$ is the softplus function $\log(1 + \exp \gamma_i)$ proposed by Dugas et al. (2001) which is fully differentiable with a derivative of $\frac{1}{1+\exp(-\gamma_i)}$. Fig.A.11 presents the behavior of the $\max[0, \gamma_i]$ function and the softplus approximation function near $\gamma_i = 0$.

Similarly to other optimization algorithms, finding one locally optimal solution with SQP is an iterative procedure. The procedure begins with an *initial guess* of link travel times and hourly passenger boardings denoted as $\boldsymbol{t}^{\delta=0}$ and $\boldsymbol{\beta}^{\delta=0}$ and generates a sequence of improved estimates until it terminates at a locally optimal solution.

SQP generates new iterates of the *initial guess*, $\boldsymbol{t}^{\delta=0}, \boldsymbol{\beta}^{\delta=0}$, by solving inequality constraint quadratic sub-problems (IQP) at each iterate δ. The idea behind the SQP solution method is to model the dispatching headways of the current iterate, $\boldsymbol{t}^{\delta}, \boldsymbol{\beta}^{\delta}$ by a quadratic programming subproblem and then use the maximizer of this sub-problem to define a new iterate, $\boldsymbol{t}^{\delta+1}, \boldsymbol{\beta}^{\delta+1}$, until convergence.

For all those inequality QP sub-problems that should be solved at each iteration, the well-known active-set method can be utilized. In the active-set method, the equality constraints are always active and the active-set is updated at any iteration by solving an equality QP where different inequality constraints are considered as active (Murty and Yu, 1988). To summarize, the maximization problem that returns the worst-case scenario for a given solution $\boldsymbol{x}^i \in \mathbf{P}$ is solved following the steps of alg.2.

Algorithm 2 Compute worst-case $\boldsymbol{t}^i$ and $\boldsymbol{\beta}^i$ for a GA population member $\boldsymbol{x}^i \in \mathbf{P}$

function MULTI-START SQP
  Set a maximum number for the multi-start solution searches $\max_{starts}$;
  for j $\in \{1, ..., \max_{starts}\}$ **do**
    Set iteration $\delta \leftarrow 0$;
    Set initial guess $\boldsymbol{t}^\delta, \boldsymbol{\beta}^\delta$ by sampling random values from the corresponding uncertainty sets $\mathcal{V}$ and $\mathcal{U}$;
    while SQP has not converged to a locally optimal solution of eq.23 **do**;
      Calculate new iterates $\boldsymbol{t}^\delta, \boldsymbol{\beta}^\delta$;
      Set iteration $\delta \leftarrow \delta + 1$;
    end while
    Return the locally optimal solution $\boldsymbol{t}^\delta, \boldsymbol{\beta}^\delta$ and set $\boldsymbol{t}^j \leftarrow \boldsymbol{t}^\delta$ and $\boldsymbol{\beta}^j \leftarrow \boldsymbol{\beta}^\delta$
    Store the value of the j^{th} locally optimal solution $\mathcal{P}(\boldsymbol{x}^i, \boldsymbol{t}^j, \boldsymbol{\beta}^j)$
  end for
  return the locally optimal solution j^* for which $\mathcal{P}(\boldsymbol{x}^i, \boldsymbol{t}^{j^*}, \boldsymbol{\beta}^{j^*}) \geq \mathcal{P}(\boldsymbol{x}^i, \boldsymbol{t}^j, \boldsymbol{\beta}^j)\ \forall j$;
  Set $\boldsymbol{t}^i \leftarrow \boldsymbol{t}^{j^*}$ and $\boldsymbol{\beta}^i \leftarrow \boldsymbol{\beta}^{j^*}$;
end function

Appendix B. Examining the solution quality in a small-scale, idealized scenario

The solution quality of our solution method can be demonstrated in a small-scale scenario because in such case a globally optimal solution can be computed with the use of simple enumeration. For this reason, we consider an idealized, small-scale scenario with only four trips for computing an optimal solution by simply evaluating all possible solutions.

Let these four trips of the small-scale scenario be the four trips of the examined bus line in Singapore, with originally planned dispatching times at 07:05, 07:10, 07:15 and 07:20 as presented in table 3. If the dispatching time modification for each trip can be in the range of $\{-3, ..., 0, ..., +3\}$ min, then the number of decision variable combinations that should be evaluated is $7^4 = 2,401$ (which means that the continuous NLP of eq.23 should be solved 2,401 times). In addition, if we assume that all other problem parameters are the same as the ones in table 2, we can compute the worst-case performance of each one of the 2,401 potential solutions and select the best-performing one. The results of this evaluation are presented in Fig.B.12a. The optimal solution with simple enumeration can be used as a benchmark for evaluating the convergence of the solution method proposed in this study. For this reason, we apply our solution method in the same idealized scenario and we report its results in Fig.B.12b.

The computation time of our solution method is 5 min and 49 sec whereas the computation time when evaluating the performance of all 2,401 decision variable combinations is 87 min and 32 sec. From the results of Fig.B.12 one can note that the computed solution with our solution method is 2.179 min (only 2.1% greater than the solution computed with simple enumeration). This indicates that our solution method exhibits a high convergence rate even if it explores a small fraction of the entire solution space. A possible explanation is the presence of multiple solutions that have a performance close to the optimal solution $\boldsymbol{x} = \{-2, -1, -1, -1\}$ min as presented in fig.B.12a.

Obviously, this analysis of the solution quality cannot be generalized to large-scale scenarios that include hundreds of daily trips. Nevertheless, it (a) indicates the convergence potential of our solution method; and (b) demonstrates the possible existence of multiple solutions close to

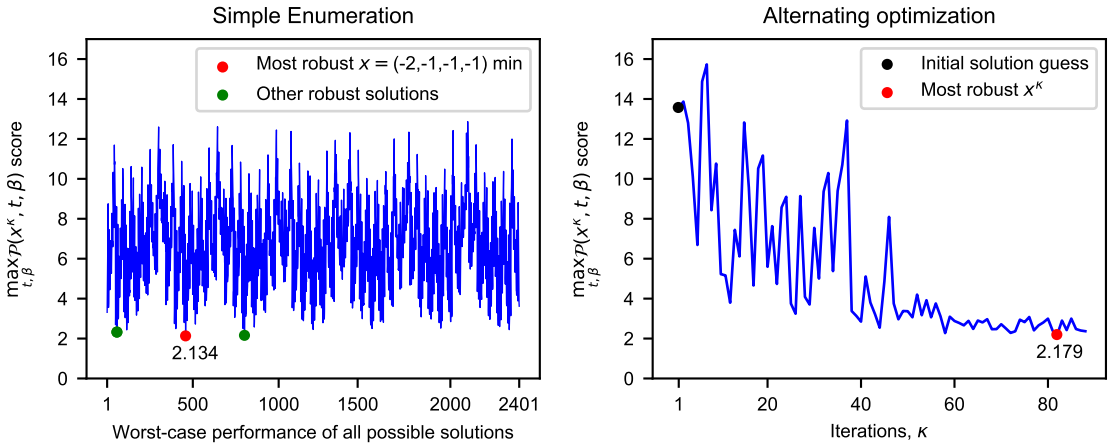

Figure B.12: (a) Optimal solution after evaluating the performance of all possible 2,401 solutions with simple enumeration; (b) Solution when using the GA and SQP solution method in the same scenario

the globally optimal one that increases the possibility of finding a (good) solution with the use of evolutionary optimization.